

92



STUDY OF THE REAL GAS EFFECTS OF NITROGEN AND AIR AT HIGH DENSITIES AND TEMPERATURES

Georges P. Rouel and Bryan E. Richards
VON KÁRMÁN INSTITUTE FOR FLUID DYNAMICS
RHODE-SAINT-GENÈSE, BELGIUM

January 1975

Final Report for Period July 1972 to September 1973

Approved for public release; distribution unlimited.

DOC_NDM SER CN
 TNC29259-PDC A 1



Prepared for

DIRECTORATE OF TECHNOLOGY
ARNOLD ENGINEERING DEVELOPMENT CENTER
ARNOLD AIR FORCE STATION, TENNESSEE 37389

NOTICES

When U. S. Government drawings specifications, or other data are used for any purpose other than a definitely related Government procurement operation, the Government thereby incurs no responsibility nor any obligation whatsoever, and the fact that the Government may have formulated, furnished, or in any way supplied the said drawings, specifications, or other data, is not to be regarded by implication or otherwise, or in any manner licensing the holder or any other person or corporation, or conveying any rights or permission to manufacture, use, or sell any patented invention that may in any way be related thereto.

Qualified users may obtain copies of this report from the Defense Documentation Center.

References to named commercial products in this report are not to be considered in any sense as an endorsement of the product by the United States Air Force or the Government.

This final report was submitted by the von Kármán Institute for Fluid Dynamics, Rhode-Saint-Genèse, Belgium, under Grant No. AFOSR-72-2413, with the Directorate of Technology, AEDC, Arnold Air Force Station, Tennessee. Mr. Elton R. Thompson, Directorate of Technology, AEDC, was the Project Scientist-in-Charge.

This report has been reviewed by the Information Office (OI) and is releasable to the National Technical Information Service (NTIS). At NTIS, it will be available to the general public, including foreign nations.

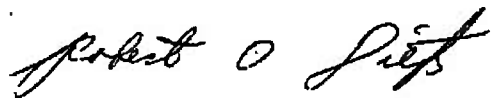
APPROVAL STATEMENT

This technical report has been reviewed and is approved for publication.

FOR THE COMMANDER



ELTON R. THOMPSON
Research and Development
Division
Directorate of Technology



ROBERT O. DIETZ
Director of Technology

UNCLASSIFIED

REPORT DOCUMENTATION PAGE		READ INSTRUCTIONS BEFORE COMPLETING FORM
1. REPORT NUMBER AEDC-TR-74-47	2. GOVT ACCESSION NO.	3. RECIPIENT'S CATALOG NUMBER
4. TITLE (and Subtitle) STUDY OF THE REAL GAS EFFECTS OF NITROGEN AND AIR AT HIGH DENSITIES AND TEMPERATURES		5. TYPE OF REPORT & PERIOD COVERED Final Report-July 1972 to September 1973
		6. PERFORMING ORG. REPORT NUMBER
7. AUTHOR(s) Georges P. Rouel and Bryan E. Richards von Kármán Institute for Fluid Dynamics Rhode-Saint-Genèse, Belgium		8. CONTRACT OR GRANT NUMBER(s) AFOSR-72-2413
9. PERFORMING ORGANIZATION NAME AND ADDRESS von Kármán Institute for Fluid Dynamics Rhode-Saint-Genèse, Belgium		10. PROGRAM ELEMENT, PROJECT, TASK AREA & WORK UNIT NUMBERS Program Element 65802F Project Numbers T-1(YA) and T-2(YB)
11. CONTROLLING OFFICE NAME AND ADDRESS Arnold Engineering Development Center (DYFS), Arnold Air Force Station, Tennessee 37389		12. REPORT DATE January 1975
		13. NUMBER OF PAGES 77
14. MONITORING AGENCY NAME & ADDRESS (if different from Controlling Office)		15. SECURITY CLASS. (of this report) UNCLASSIFIED
		15a. DECLASSIFICATION/DOWNGRADING SCHEDULE N/A
16. DISTRIBUTION STATEMENT (of this Report) Approved for public release; distribution unlimited.		
17. DISTRIBUTION STATEMENT (of the abstract entered in Block 20, if different from Report)		
18. SUPPLEMENTARY NOTES Available in DDC		
19. KEY WORDS (Continue on reverse side if necessary and identify by block number) thermodynamics of real gases entry vehicles high density gas properties intermolecular forces high temperature gas properties vibrational excitation research facilities and instrumentation		
20. ABSTRACT (Continue on reverse side if necessary and identify by block number) A free piston compression tube has been used to generate samples of nitrogen and air test gases pressures up to 3000 kg/cm² and 2300°K. A description of the measurement of pressure, temperature and volume (driving part of the cycle) has been made. The techniques used are piezo-electric transducers, a sodium line reversal technique and an eddy-current transducer, respectively. Calculations and experiments have been carried out which have		

UNCLASSIFIED

UNCLASSIFIED

20. ABSTRACT (Continued)

indicated that the level of uncertainty of measurement of these parameters is below $\pm 5\%$ at peak conditions and within $\pm 10\%$ at conditions away from the peak. The results of the experiments in nitrogen have shown that agreement with the equation of state at low conditions is i.e. 1700°K and 1400 kg/cm^2 good, but a systematic deviation from that expected is obtained at higher conditions. The deviations from that expected from published tables describing the thermodynamic state of air are found to be large, but these may be due to a problem of contamination caused by the reactive nature of hot, high pressure oxygen.

PREFACE

This technical report was prepared by the von Kármán Institute for Fluid Dynamics, Rhode-Saint-Genèse, Belgium, under Grant No. AFOSR-72-2413, Program Element 65802F, for the Directorate of Technology, Arnold Engineering Development Center (AEDC), Air Force Systems Command (AFSC), Arnold Air Force Station, Tennessee. The work was conducted from July 1972 to September 1973 with Mr. Elton R. Thompson, Directorate of Technology, AEDC, acting as Project Scientist.

The authors would like to acknowledge Professor K. R. Enkenhus, now of the Naval Ordnance Laboratory, who was mainly responsible for the theoretical aspects of the work and Professor M. J. Lewis, now of the Institute für Reaktorforschung, Switzerland, who was mainly responsible for the experimental aspects. The assistance of technical engineers Jean Hugé, Roger Borrès, Roger Conniasselle, and their assistants is greatly appreciated.

The reproducibles used in the reproduction of this report were supplied by the authors.

TABLE OF CONTENTS

1. INTRODUCTION	5
2. EXPERIMENTAL TECHNIQUE	7
2.1 The test gas compression system	7
2.2 Pressure instrumentation	9
2.3 Temperature instrumentation	9
2.4 Extension of the range of temperature measurement beyond 2500°K	15
2.5 Density measurement	16
2.6 Compression cycle measurement control system	19
2.7 Typical results	19
3. COMPUTER PROGRAM AIDS TO THE EXPERIMENTS	22
3.1 Piston compression cycle predictions	22
3.2 Data reduction programs	24
4. CALIBRATION PROCEDURES	28
4.1 Pressure measuring equipment	28
4.2 Lamp and optical system	30
4.3 Recording equipment	35
4.4 Photomultipliers	37
4.5 Position measurements	37
5. DISCUSSION OF UNCERTAINTIES	38
5.1 Justification of using a "dynamic" experiment to measure thermodynamic state	38
5.2 Pressure variations in the gas sample	40
5.3 Assessment of temperature variations in the gas sample	40
5.4 Experimental study of spatial uniformity of pressure in the test chamber	42
5.5 Experimental assessment of wall heat transfer during a test	44
5.6 Gas leakages	46
5.7 Contamination of the gas	46
5.8 Initial temperature of the test gas	47
5.9 Summary of measurement uncertainties	48

6. RESULTS AND DISCUSSION 49

 6.1 Measurements in nitrogen 49

 6.2 Measurement in air 61

7. CONCLUSIONS 72

8. FUTURE EXTENSIONS OF THE RESEARCH 73

 8.1 Interpretation of data 73

 8.2 Extension of experiments to cover a larger
 temperature and entropy range in nitrogen . 74

 8.3 Diagnosis of the large deviations from
 equation of state of experiments in air . . 75

 8.4 Theoretical survey for an appropriate
 equation of state for air 75

REFERENCES 76

INTRODUCTION

Aerodynamic ground test facilities for simulating re-entry flows involve the use of very high operating pressures at high temperatures (Ref.1). Under these conditions the equation of state departs markedly from the perfect gas law due to compressibility effects and excitation of internal energy modes. The associated thermodynamic properties are hence also strongly influenced. Optimisation studies of ground test facilities require that such gas imperfections are known with a reasonable degree of accuracy. This report describes an experimental program to make accurate measurements of pressure, volume and temperature of nitrogen and air at pressures up to 3000 kg/cm² and temperatures up to 2500°K, a range of conditions in which the compressibility effects are most dominant.

The behaviour of dense gases may, in principle, be predicted using quantum-statistical mechanics. However, the mathematical difficulties involved when molecular interactions must be taken into account are so formidable that solutions have only been found using highly simplified molecular models (Ref.2). Many attempts have been made to obtain semi-empirical equations of state which are valid for any dense gas by the application of Van der Waals' principle of corresponding states (Refs 3 and 4). These depend on having available knowledge of the equations of state over the range required. Once the equation of state is defined, all thermodynamic properties can be obtained from existing relations (Ref.4).

Up to present experiments, providing the knowledge on which the equations of state are based, have been confined to the studies of gases at high pressures and ordinary

temperatures, where measurements may be made under steady state conditions. A large amount of data is available in this regime. The contrary is true at high temperatures because of the problems encountered in maintaining the structural integrity of the containing vessel. These problems can be overcome by rapidly heating and compressing a gas sample by a piston, and taking the desired measurements under transient conditions. Work of this kind has been carried out in the USSR, but aside from a brief monograph on the experimental equipment and techniques employed (Ref.5), no results seem to have been subsequently published in the open literature.

The driver section of the VKI Piston Driven Shock Tube has been modified to generate samples of dense high temperature gases and instrumentation has been developed to measure pressure, temperature and density (Ref.6). A sodium spectral line reversal technique is used to measure the temperature of the gas. The density of the gas is determined indirectly, by measuring the piston's position during the compression process. This measurement involves the use of an eddy current displacement transducer. A quartz-crystal piezo electric transducer is used to measure the pressure of the gas. More details of the instrumentation are given within. A full description of the VKI Piston Driven Shock Tube and its control equipment before conversion to a compression tube is given in Ref.7.

The report describes experiments carried out to generate thermodynamic state data of nitrogen and air and to assess the experimental accuracy. The results are compared with published thermodynamic tables.

2. EXPERIMENTAL TECHNIQUE

2.1 The test gas compression system

The system for compressing the gas is illustrated in Fig.1. A piston constructed of hardened steel, aluminium and nylon, weighing 12.6 kg and of length 250 mm is free to move in a barrel of 12.8 mm diameter and 1.98m in length. The barrel is attached to a reservoir, of diameter 270 mm and length 2.3m at one end and is closed at the other end. Initially an aluminium diaphragm, typically of thickness 0.4 mm, retains the piston at the reservoir end of the barrel. The gas under test is introduced into the barrel after evacuating and purging the barrel with the use of a vacuum pump^x, and the reservoir is charged with air up to its operating pressure P_0 at temperature T_0 . To release the piston at a selected time, the reservoir gas is bled in such a way as to act on a larger area of the piston rear surface, the extra force generated being adequate to shear the retaining diaphragm. Subsequently the piston is driven down the barrel compressing the test gas from an initial pressure P_{4_i} and T_{4_i} to a maximum pressure P_{4_f} and temperature T_{4_f} . Both T_0 and T_{4_i} are equal to the laboratory temperature. The piston is instantaneously at rest when the peak pressure is achieved. After the first compression stroke, the piston reverses its motion and returns to the reservoir end of the barrel. It continues to oscillate in the barrel until brought to rest by friction. Values of P_{4_f} up to 3000 kg/cm² can be achieved depending on the initial pressure ratio across the piston. This limitation is imposed by the strength of the barrel and its end fittings.

^x Leybold vacuum diffusion pump (type PD 1000/635) and a rotary "backing" pump (Type D12 156/16).

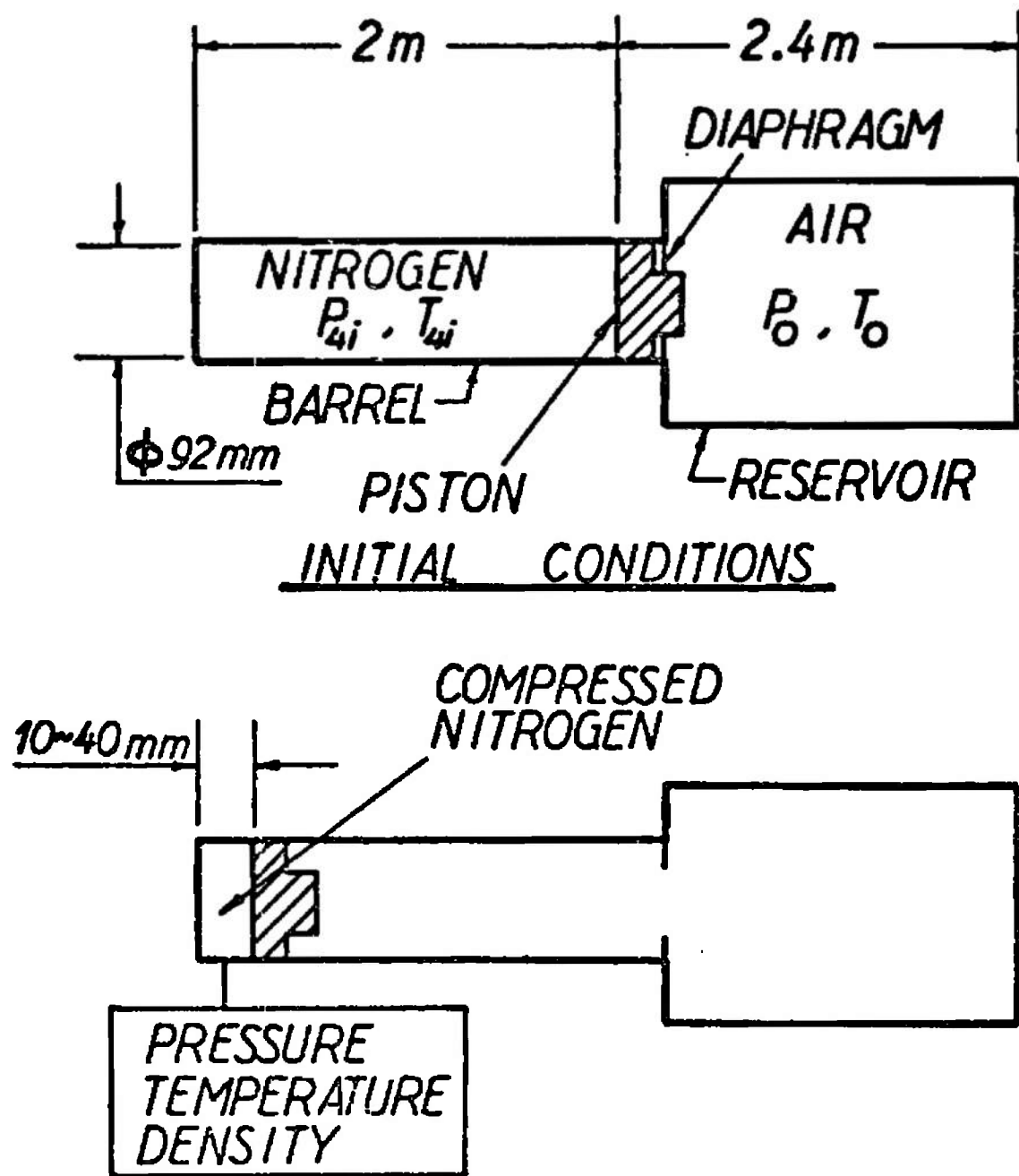


FIG. 1 Schematic of gas compression system.

The pressure (P_4), temperature (T_4) and density (ρ_4) variations of the nitrogen are measured during the first compression stroke. Typically, the initial barrel pressure measured by means of either a mercury manometer or a Wallace and Tiernan gauge is 1 kg/cm^2 ; the transit time of the piston from its initial rest position to its "peak pressure" rest position is about 50 msec. The total measurement time of interest is of the order of 1 msec. During this time, the piston is between 10 and 40 mm from the closed end of the barrel.

The facility and its instrumentation are shown in Fig.2.

2.2 Pressure instrumentation

The pressure variation of the test gas during the compression is measured using either a Type 6221 or Type 6201 Kistler piezo-electric pressure transducer and a Kistler 568/M5 charge amplifier and recorded on a Tektronix Type 502A Oscilloscope. The transducer is mounted in the wall and near the end of the barrel, as depicted in Fig.3. The oscilloscope trace is photographed with a Polaroid camera.

2.3 Temperature instrumentation

The temperature of the test gas is determined by using the sodium-line reversal technique (Ref.8). A single source effective double beam system, shown schematically in Fig.4 is used. Two back silvered prisms are mounted in the end wall of the barrel, forming a small enclosure into

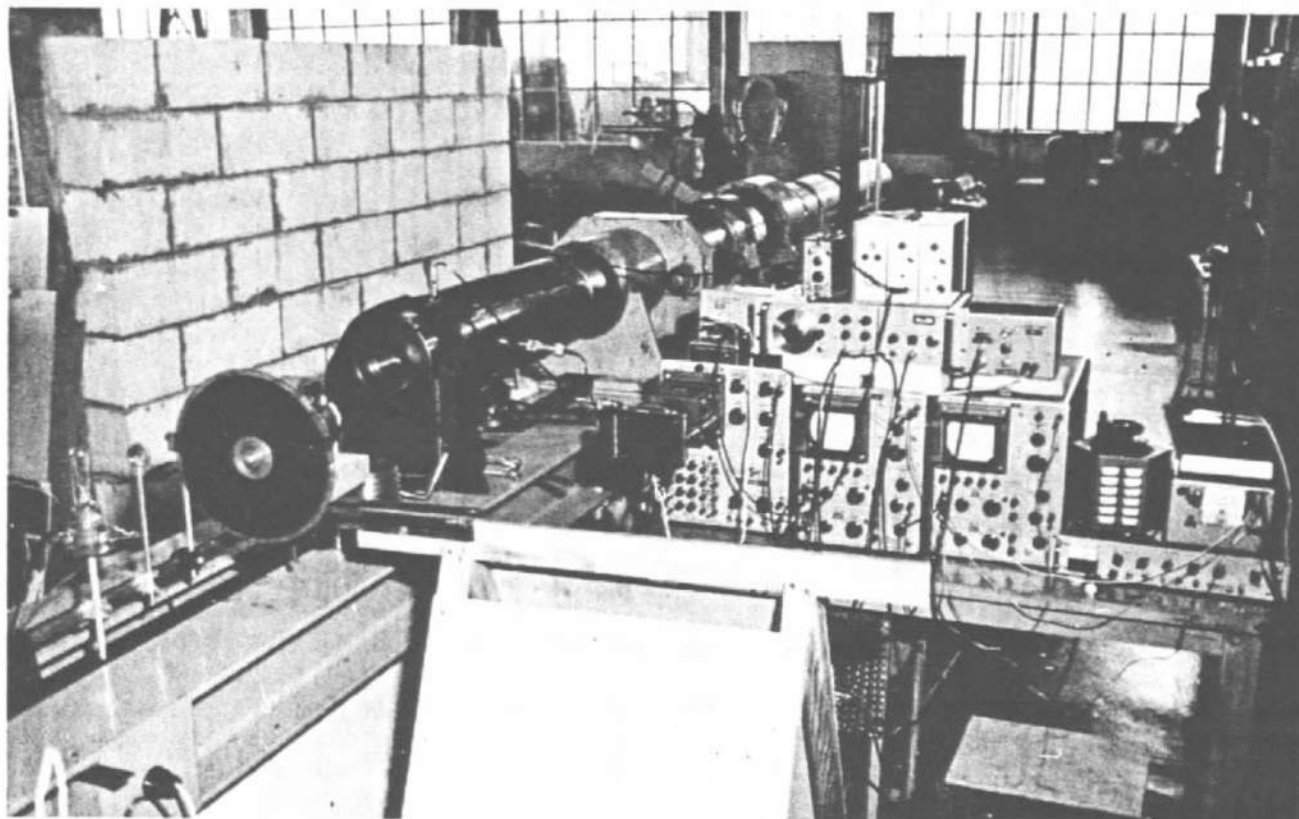


FIG. 2 Photograph of facility.

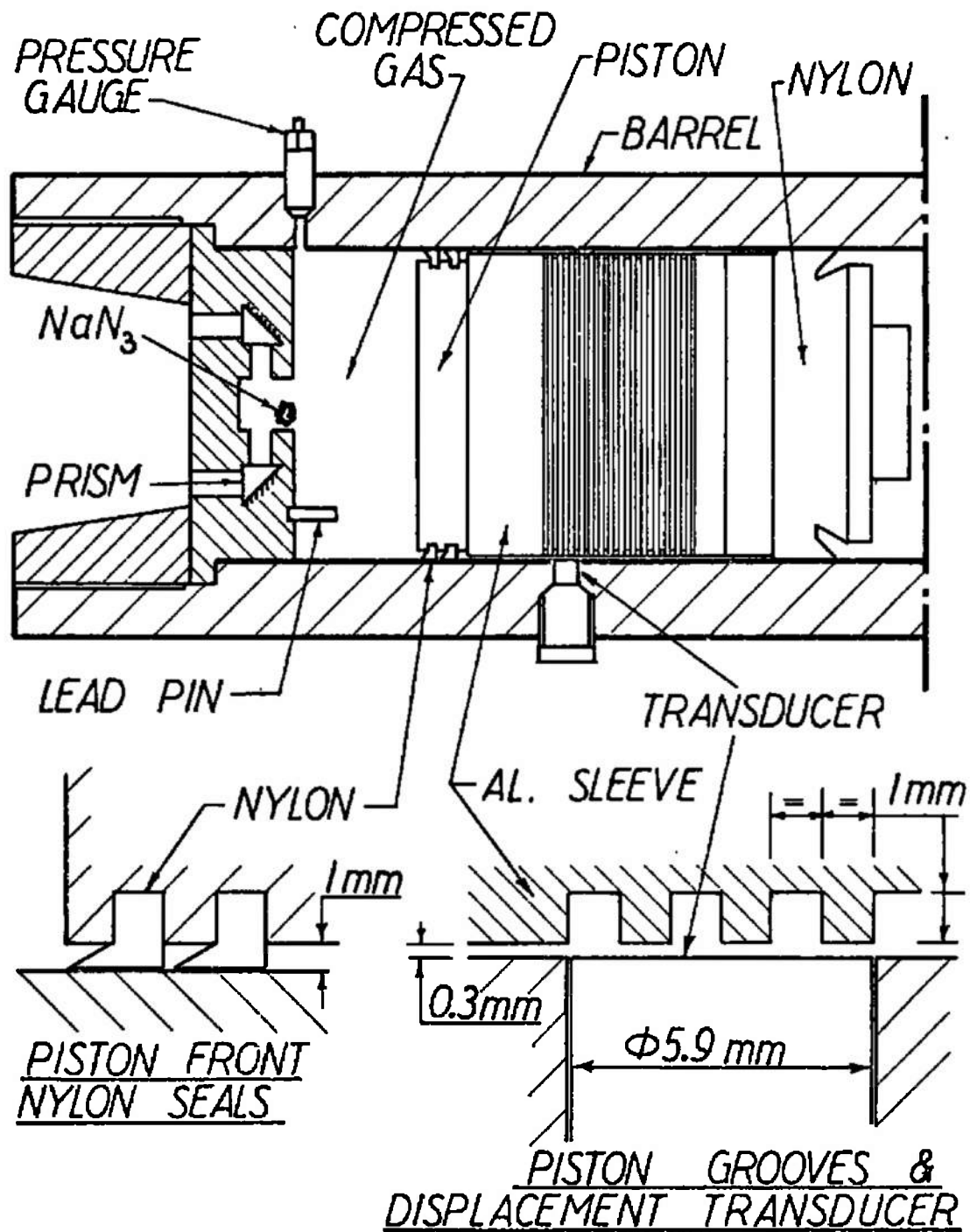


FIG. 3 Schematic of test section of compression tube illustrating the instrumentation position.

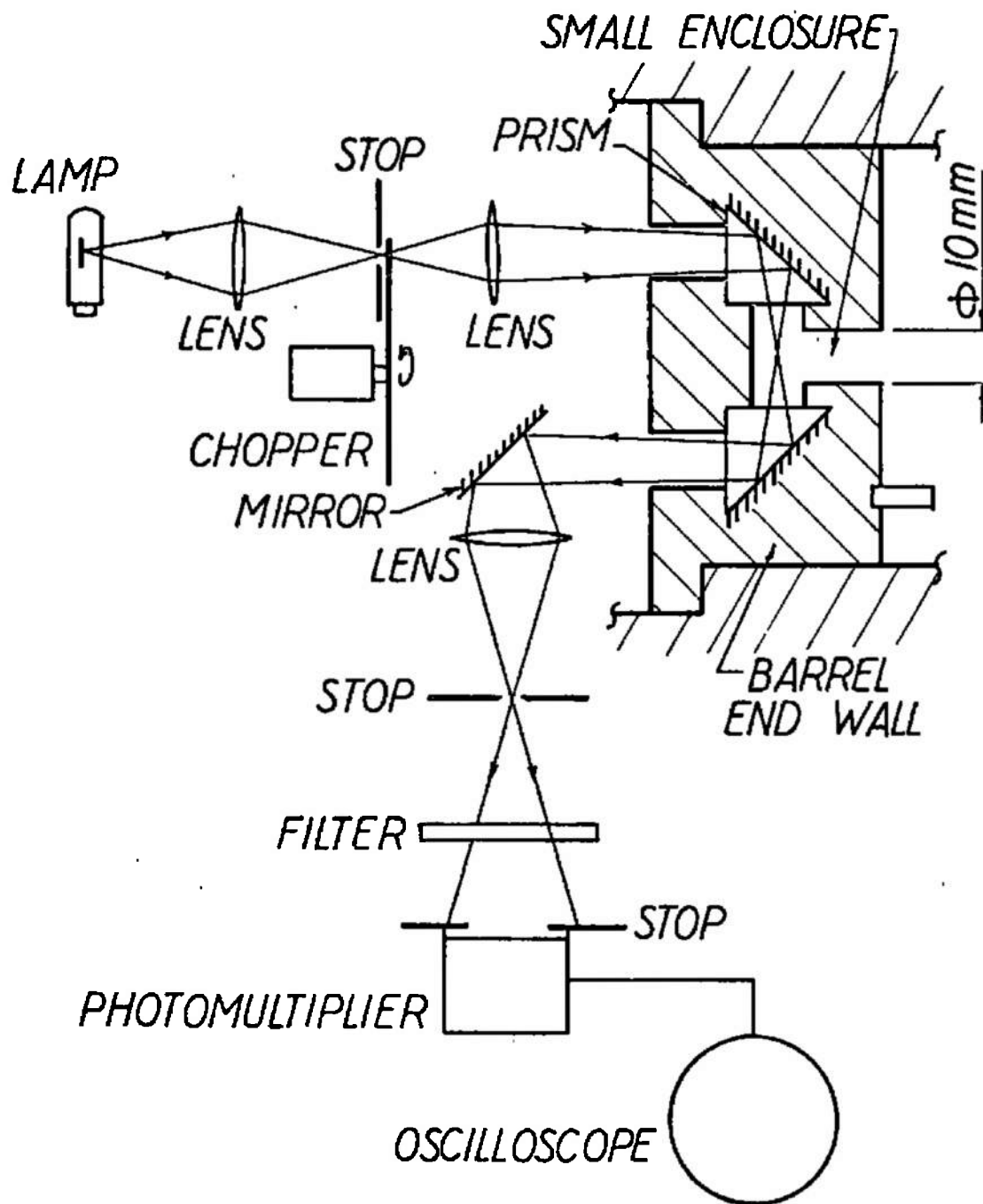


FIG. 4 Sodium line reversal optics.

which some of the nitrogen test gas is compressed during the compression stroke (see Fig.3). Light from a tungsten strip-filament lamp is modulated by a mechanical chopper and is focused by a lens system and directed by one of the prisms into the enclosure. The light passes out of the enclosure by means of the second prism. A mirror and lens system direct the light to an EMI 9558C photomultiplier. Suitable stops limit the solid angle and the enclosure volume monitored by the photomultiplier. The signal from the photomultiplier is recorded on the second channel of the Tektronix 502A oscilloscope.

The test gas is seeded with sodium atoms by placing a few milligrams of sodium azide, NaN_3 , at the entrance of the enclosure. Sodium azide decomposes exothermically at 600°K to form free sodium atoms and nitrogen (Ref.9). Hence during the compression process, sodium atoms are formed, raised to a high temperature, and compressed into the small enclosure. At temperature above 1200°K , the atoms emit light at characteristic wavelengths and this light is monitored by the photomultiplier.

The principle of the sodium line reversal technique is briefly as follows. When light from the lamp is present, and provided that its intensity is greater than the intensity of the thermal emission from the sodium atoms^x, these atoms will absorb some of the light from the lamp. By comparing the absorption and emission of the sodium atoms with the intensity of the light emitted by the lamp, the "electronic" temperature T_g , of the sodium atoms is determined from the statically calibrated brightness temperature T_L , of the lamp. The relevant equations and assumptions governing the use of the technique are presented by Lapworth (Ref.10).

^x This is always the case in the present experiments. If the contrary occurs, the reversal technique, as used here, becomes a very inaccurate thermometer (Ref.11).

In the present experiments, the spectral region of interest, namely, the sodium D-line doublet, is isolated by a filter which has a half-band width of 40 Å centred about a wavelength of 5895 Å. If v_1 is the photomultiplier output voltage when the lamp light is cut off by the chopper, v_2 is the voltage when no sodium atoms are present and only the lamp light is monitored and v_3 is the voltage when both the light from the lamp and the sodium atoms is recorded, then T_s may be determined (Ref.11) from

$$\frac{1}{T_s} = \frac{1}{T_L} + \frac{k}{h\nu} \ln\left(1 + \frac{v_2 - v_3}{v_1}\right) \quad (1)$$

where k is the Boltzmann constant, h the Planck constant and ν the central frequency of the sodium D-lines. v_1 is a measure of the intensity of the thermal emission from the sodium atoms alone, v_2 is a measure of the intensity of the lamp light and v_3 is a measure of the emission of the sodium atoms and the absorption of these atoms relative to the light from the lamp. v_2 is recorded prior to the compression stroke, v_3 and v_1 may be measured almost simultaneously, provided the lamp light chopping frequency is sufficiently high. Hentall et al (Ref.12) show that the electronic temperature of the sodium atoms is equal to the vibrational temperature of the nitrogen.

Under the present high pressure, high temperature circumstance, the vibrational energy relaxation time of the gas is of the order of 0.1 μs. Therefore, the test gas is undoubtedly in equilibrium during the compression cycle and the equilibrium temperature variation of the gas is determined. The line reversal technique as used here can be shown to measure the test gas temperature with an uncertainty of less than two percent (Ref.11) provided T_L is always greater

than T_s .

The sensitiveness of the measurement is illustrated by the fact that at 2500°K for the sodium wavelength a factor of two in light intensity corresponds to a change of only 160° in temperature i.e. around 6 per cent (Ref.8).

2.4 Extension of the range of temperature measurement beyond 2500°K

Some research effort has been applied to selecting an accurate method of measuring the temperatures above the 2,500°K limit imposed by the use of a tungsten ribbon lamp. Two methods are chosen to be most appropriate.

i) Sodium-line reversal technique using a carbon arc source

Null and Lozier (Ref.13) have reviewed the use of a carbon arc source as a radiation standard. Positive electrode crater temperatures of 3,800°K can be achieved and maintained with a reproducibility of $\pm 10^\circ\text{K}$. The spectral radiance appears close to that typical of a black body of 3,800°K over most of the visible range, but particularly in the vicinity of the sodium D-line. The spectral emissivity of the crater approaches unity over this desired spectral range. This light source enables the existing sodium line reversal optical components to be used to extend the range to about 3,500°K. This source is a constant temperature device, and filters have to be used to decrease the effective temperature to lower values. A high pressure xenon arc lamp was also considered, however, considerable difficulties are anticipated in its calibration because its spectral distribution is not close to that of a black body.

ii) Infra-red technique

In this technique, the response of an infra-red sensor (such as a fast response photo-conductive indium antimonide detector cooled by liquid nitrogen) to a black-body source radiation passing through the test gas is used to measure the gas temperature (Ref.3). An advantage of this system over the sodium line reversal technique is that the introduction of an appropriate seed material, carbon monoxide, into the test gas is simpler to control. Furthermore, the temperature range is much greater (less than 600°K to greater than 4,000°K is claimed by Lapworth in Ref.14). An appropriate black body source is described in Ref.15. An accuracy of 2% up to a temperature of 4,000°K is claimed for this technique, but for low pressure conditions.

The first technique has been selected for this work for two reasons. No experience has been obtained in the use of infra-red techniques at the Institute. Furthermore, none of the equipment necessary for the technique exists here.

A suitable carbon-arc source manufactured by Spindler and Hoyer, Germany has been selected and received. Experience in the use of the equipment is being amounted for the future extension of the work close to 3,500°K.

2.5 Density measurement

The density variation of the compressed nitrogen is determined from accurate measurements of the piston's position relative to the barrel during the final stages of the compression stroke.

Two complementary systems are used. A small lead pin, mounted in the end wall of the barrel, is crushed by the piston. The length of the crushed pin gives the displacement L of the piston from the end wall at peak pressure. Away from peak pressure, the piston's position is monitored at intervals of one millimeter by a displacement transducer mounted in the side of the barrel. The pin and transducer positions are shown in Fig.3. The latter's position prevents the transducer from being subjected to pressure levels above 30 kg/cm^2 . The transducer, a commercially available Vibrometer TW6-100/A eddy-current contactless displacement transducer, monitors accurately machined grooves on an aluminium sleeve attached to the piston. The transducer is excited by a Vibrometer type 100 TRI/A carrier amplifier. The operation of the transducer is illustrated in Fig.5.

Knowing the piston position relative to the transducer, the displacement (L) and volume (V_4) of the compressed gas may be determined from the geometry of the barrel and piston. The number of moles M , of gas in this volume is known from a measurement of the initial volume V_{4i} , pressure P_{4i} , and temperature T_{4i} . The density of the gas is given by

$$\begin{aligned} \rho_4 &= \frac{M}{V_4} \\ &= \frac{P_{4i} V_{4i}}{\bar{R} T_{4i} V_4} \end{aligned} \quad (2)$$

where \bar{R} is the gas constant per mole. In deriving Eq.2, it is assumed that no gas leaks past the piston during the compression stroke.

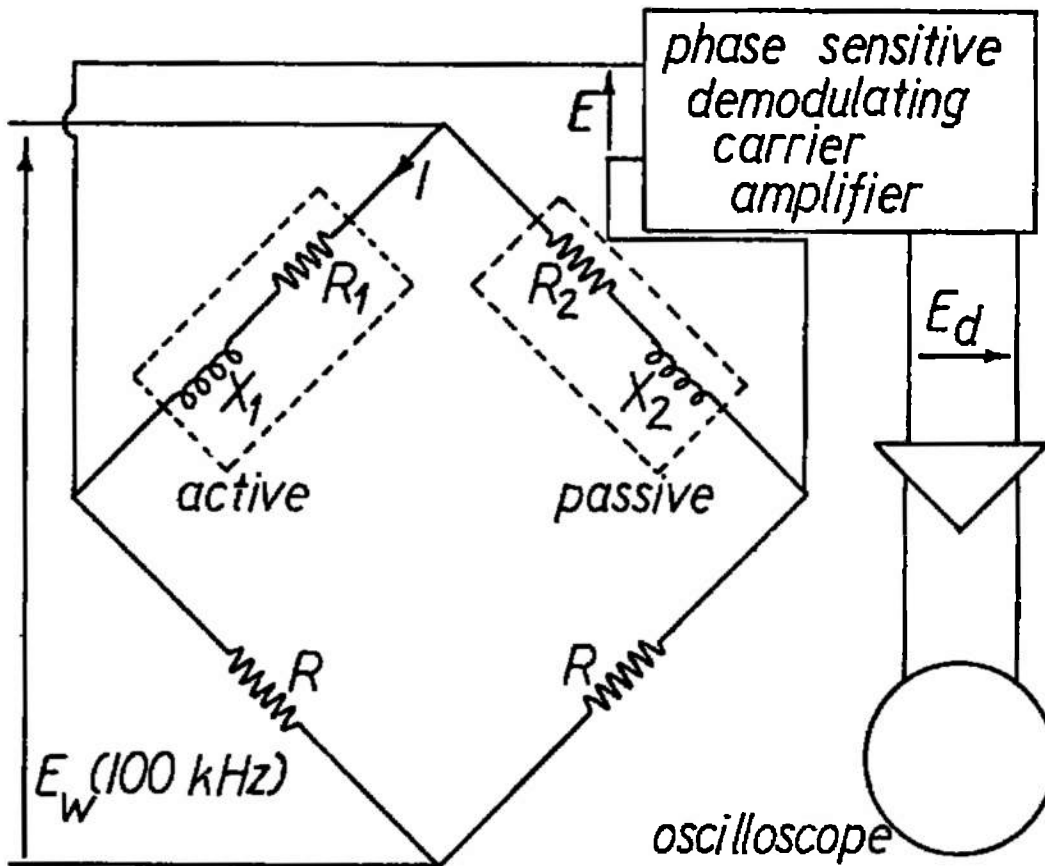
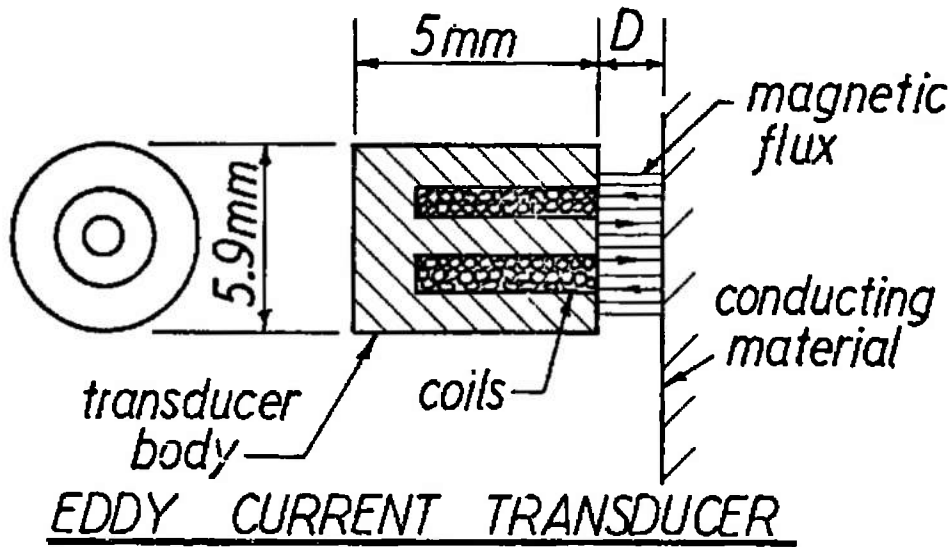


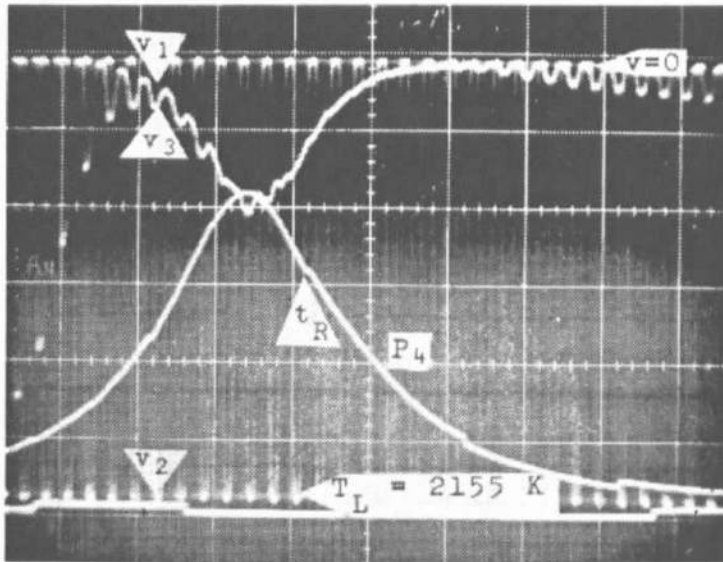
FIG. 5 Displacement transducer.

2.6 Compression cycle measurement control system

During the final stages of the piston compression stroke, the pressure, temperature and piston position signals are recorded simultaneously. The output from the position transducer triggers the sweep of the oscilloscopes. The vertical amplifier of the Tektronix type 531A oscilloscope used to record the position measurement operates in the d-c mode and is adjusted so that a signal is recorded only when the grooves on the piston are traversing the transducer. The time scale of the trace is extended by using the four alternate trace capability of the oscilloscope's type M plug-in unit. A four trace "raster" display, which has a calibrated sweep-back time of 30 μ s, is obtained. The oscilloscope monitoring pressure and temperature signals operates in the single-sweep mode to prevent recording compression strokes other than the first. Base lines on the traces are added just before each test. To correlate the time scales of the two oscilloscopes, a one-kHz square wave of small amplitude is superimposed upon the pressure measurement and piston position measurements signals.

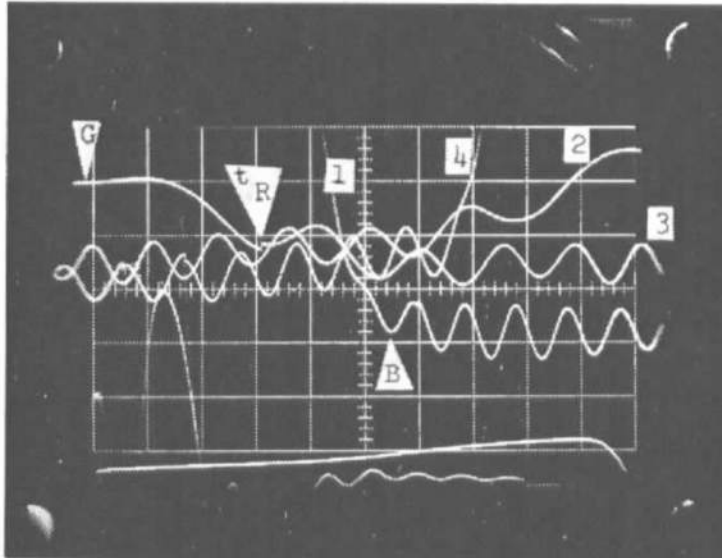
2.7 Typical results

A compression test was carried out with the following initial conditions : $P_0 = 30 \text{ kg/cm}^2$, $T_0 = 292^\circ \text{K}$, $P_{4_i} = 1,285 \text{ kg/cm}^2$ and $T_L = 2,155^\circ \text{K}$. The oscillograms obtained from this test are shown in Figs 6 and 7. On the temperature and pressure oscillogram, typical values of v_1 , v_2 and v_3 are indicated, together with the photo-multiplier signal ($v = 0$) corresponding to the zero light level. Point B on the position measurement oscillogram corresponds to the time when the centre of the first "tooth" on the piston arrived at the centre of the transducer. At this time, the distance L from the front



Horizontal sensitivity = 250 μ s per square
 Pressure, vertical sensitivity = 525 kg/cm² per square
 Temperature, vertical sensitivity = 0.5V per square

FIG. 6 Oscillogram of pressure and temperature.



Horizontal sensitivity = 50 μ s per square
 Vertical sensitivity = 1V per square

1 - First trace 3 - Third trace
 2 - Second Trace 4 - Fourth trace

FIG. 7 Oscillogram of position.

face of the piston to the end wall of the barrel was 35.5 mm. Each subsequent "maximum" and "minimum" corresponds to the piston moving one millimeter closer to the barrel end wall. The piston rest position at peak pressure is indicated by point G on the oscillogram. L is there given by the length (10.59 mm) of the crushed lead pin. After point G, the maxima and minima on the trace give the piston's position at intervals of one millimeter as the piston moves away from the end wall. Point G on the trace is determined from the centre of symmetry of the position transducer signal. Typical time marks from the one-kHz square wave, superimposed on the pressure and position measurement signals, are indicated by point t_R on each oscillogram. At these points, an exact correlation in time, between the oscillogram traces, is obtained. Away from these times, the signals are correlated by using the accurately calibrated time scales of the oscilloscopes.

3. COMPUTER PROGRAM AIDS TO THE EXPERIMENTS

3.1 Piston compression cycle predictions

Calculations concerning the compression of the gas have been carried out using a piston cycle program. The basic program uses a 4th order Runge-Kutta numerical method to solve the system of two ordinary differential equations resulting from Newton's law describing the forces on the piston, including friction during the cycle. The program has been modified in the following several ways providing aids to the estimation of various sources of uncertainty.

The gas in front of and behind the piston is assumed to be in an isentropic state during the cycle. This assumption is possible if no shock waves are generated in the flow. The pressure traces exhibit no sudden jumps indicative of shock waves. The accuracy of this assumption was examined by modifying the program to calculate the heat losses from the gas sample during the test assuming that heat conduction was the only mechanism of heat transfer. The method of Knöös (Ref.16) was used. Results of this program are discussed in section 5.3.

The pressure of the gas behind the piston was always low enough that an assumption of a perfect gas could be made. It was verified also that the flow behind the piston could be assumed to have infinite speed of sound provided that the piston speed never exceeded about one third of local sound speed. Several calculations carried out using the full characteristics solution behind the piston showed that less than 1% departures are incurred by this latter assumption.

The equation of state used to calculate the behaviour of the test gas in front of the piston was the

Enkenhus-Culotta (Ref.4) equation for nitrogen and the Grabau-Brakinsky (Ref.17) tables for air. Again an assumption of infinite speed of sound was used. This assumption was examined by modifying the program to calculate the behaviour of the compressed gas using the full characteristics solution, but assuming a perfect gas. Computer limitations prevented carrying out this calculation using a valid real gas equation of state, but the conclusions of the estimations would not be expected to be altered by using the simpler equation of state model. Again it was shown that less than 1% departures were obtained assuming infinite speed of sound in the compressed test gas for low piston speeds.

The piston friction provides an important practical consideration in evaluating the performance of the facility. It is not however an important consideration concerning the measurements of the state of the gas since all three parameters, p , ρ , T which define the thermodynamic state are measured simultaneously. The chief source of friction is expected to arise from the flexible piston seals used to ensure no leakages. A feature of the experiments to generate equation of state data is that leakages provide a source of experimental error since the time dependent density variation is calculated not only from the measured piston motion but also from an assumption of constant mass of test gas during the cycle. In the piston cycle program, it was assumed that the friction was independent of piston velocity, but is a function of both the pressure in front and behind the piston. These pressures act on the flexible seal. Various values of friction coefficients were examined. The consideration of friction causes a slight asymmetry in the thermodynamic measurements during the compression and the expansion caused by the rebound of the piston.

The various forms of the program were used to aid the carrying out of the experiments as well as to make assessments of uncertainties. Results from the program are mentioned in later sections of the report.

3.2 Data reduction programs

Two main data reduction programs have been designed. One program uses inputs of the measurements of the traces as read directly from the measuring table and all the carefully determined calibration constants to calculate the raw data. The second program presents the results to allow comparison with appropriate equations of state.

1. Data reduction of raw data

The values of the state parameters are generated by introducing into the program the co-ordinates of the pressure, emission, absorption and position traces. The first three are introduced at equal time intervals; the latter is introduced as the time, arbitrarily referenced, for the distance transducer to sense the equal interval distances defined by the centre of the teeth and the grooves of the piston.

The following information, the acquisition of which is described in a following section, is also provided :

- oscilloscope and transducer calibration curves and values,
- lamp voltage and current, and lamp characteristic curve,
- transmission coefficients of the optical system,
- crushed lead pin length,
- corrections for barrel expansion and piston compression due to the high pressures developed.

The data is then re-arranged in equal interval time steps by using a four-point interpolation formula. A typical computer read out of the program is shown in Table 1.

2. Comparison between experimental data and theoretical equation of state

A computer program was devised to aid the comparison of theoretically determined equations of state with the experimental results. It calculates for each measured point (P, ρ, T) the following parameters : $P_{\text{calc}}(\rho_{\text{meas}}, T_{\text{meas}})$ i.e. calculated pressure from measured density and measured temperature; $\rho_{\text{calc}}(P_{\text{meas}}, T_{\text{meas}})$; and $T_{\text{calc}}(P_{\text{meas}}, \rho_{\text{meas}})$. Also the entropies $S_1/R(\rho_{\text{meas}}, T_{\text{meas}})$, $S_2/R(P_{\text{meas}}, T_{\text{meas}})$, $S_3/R(P_{\text{meas}}, \rho_{\text{meas}})$ are calculated.

The theoretical thermodynamic information used for nitrogen was the Enkenhus-Culotta equation of state (Ref.4) which agrees with the AEDC tables (Ref.18) to within a few per cent for all parameters over the range considered. Two subroutines give pressure and dimensionless entropy as a function of density and temperature. For air, the AEDC tables (Ref.17) were used. A four point interpolation formula gives pressure and dimensionless entropy as a function of density and temperature. In each case a Newton-Raphson searching procedure is used to calculate ρ_1 , T_1 , S_2/R and S_3/R when the arguments are not density and temperature.

The overall uncertainty in percent is also given. A typical computer read out is given in Table 2.

TABLE I. Computer Read-Out of Programme 1 (Data reduction).

AEDC-TR-74-47

RUN NUMBER 39GAS#AIR						RUN NUMBER 39GAS#AIR					
TIME	+OR-	PRES	+OR-	TEMP	+OR-	TIME	+OR-	RHO	+OR-	LAMBDA	POSITION
MUSEC		KG/CM2		K		MUSEC		AMGT		MM	MM
-1090.3	11.	225.5	3.	1481.2	13.	-1413.3	14.	37.5	0.1	44.0	44.12
-1039.5	10.	240.4	3.	1510.2	14.	-1387.7	13.	38.4	0.1	45.0	43.12
-988.7	9.	258.1	3.	1543.7	14.	-1353.2	13.	39.3	0.1	46.0	42.12
-937.8	9.	273.0	3.	1577.6	15.	-1317.7	13.	40.2	0.1	47.1	41.12
-887.0	8.	291.7	3.	1619.3	16.	-1289.4	12.	41.2	0.1	48.3	40.12
-836.2	8.	314.0	3.	1648.2	17.	-1255.2	12.	42.2	0.1	49.5	39.12
-785.3	7.	338.2	3.	1665.2	17.	-1223.0	12.	43.3	0.1	50.8	38.12
-734.5	7.	358.6	3.	1672.4	17.	-1188.8	11.	44.5	0.1	52.1	37.12
-683.7	6.	385.6	3.	1680.0	17.	-1155.3	11.	45.7	0.1	53.5	36.12
-632.8	6.	413.4	3.	1703.5	18.	-1121.1	11.	47.0	0.1	55.0	35.12
-582.0	5.	443.1	3.	1737.4	19.	-1088.2	10.	48.3	0.1	56.6	34.12
-531.2	5.	472.8	3.	1735.3	19.	-1057.6	10.	49.8	0.1	58.3	33.12
-480.3	4.	509.8	3.	1704.9	18.	-1018.2	10.	51.3	0.1	60.1	32.12
-429.5	4.	546.0	3.	1692.2	17.	-964.9	9.	53.0	0.1	62.0	31.11
-378.7	3.	579.4	3.	1704.2	18.	-931.4	9.	54.7	0.1	64.1	30.11
-327.8	3.	618.3	3.	1731.1	18.	-893.9	9.	56.6	0.1	66.3	29.11
-277.0	2.	655.3	3.	1798.3	21.	-859.0	8.	58.6	0.1	68.6	28.11
-226.2	2.	692.4	3.	1815.6	22.	-815.0	8.	60.8	0.1	71.2	27.11
-175.3	1.	721.9	3.	1826.3	30.	-778.8	7.	63.1	0.1	73.9	26.11
-124.5	1.	750.6	3.	1836.7	14.	-735.4	7.	65.6	0.1	76.9	25.11
-73.7	0.	775.5	3.	1844.2	17.	-692.3	6.	68.4	0.1	80.1	24.11
-22.8	0.	789.4	3.	1850.4	18.	-645.7	6.	71.3	0.2	83.6	23.11
						-596.7	6.	74.6	0.2	87.4	22.11
						-550.3	5.	78.2	0.2	91.7	21.11
						-496.7	5.	82.2	0.2	96.4	20.11
						-445.8	4.	86.7	0.2	101.6	19.11
						-365.9	3.	91.8	0.2	107.5	18.11
						-298.8	3.	97.5	0.3	114.2	17.11
						-214.0	2.	104.0	0.3	121.8	16.11
						-98.9	0.	111.5	0.3	130.6	15.11
						78.9	0.	119.7	0.3	140.2	14.12

TABLE 2. Computer Read-Out of Programme 2 (Comparison between experiment and thermodynamic data).

RUN NUMBER 39			HVR7207								
P	R	T	P(R,T)	R(P,T)	T(R,P)	S(R,T) S(P,T) S(P,R)					
KG/CM2	AMGT	K	KG/CM2	AMGT	K						
225.5	48.2	1481.2	289.7	28.4	38.1	-20.9	1156.6	-21.0	24.30	24.55	23.51
240.4	50.5	1510.2	310.5	29.1	39.7	-21.3	1173.4	-22.2	24.31	24.57	23.51
258.1	52.2	1543.7	328.6	27.2	41.6	-20.2	1216.3	-21.2	24.35	24.60	23.58
273.0	54.4	1577.6	351.1	28.5	43.0	-20.9	1230.7	-21.9	24.38	24.63	23.57
291.7	57.0	1619.3	379.2	30.0	44.6	-21.6	1249.6	-22.8	24.42	24.68	23.56
314.0	59.7	1648.2	406.2	29.3	47.0	-21.2	1278.2	-22.4	24.43	24.68	23.58
338.2	62.7	1665.2	432.9	28.0	49.9	-20.3	1304.7	-21.6	24.41	24.65	23.59
358.6	65.7	1672.4	457.6	27.5	52.5	-20.0	1314.5	-21.4	24.37	24.62	23.56
385.6	68.9	1686.0	486.5	26.1	55.7	-19.1	1339.7	-20.5	24.34	24.58	23.57
413.4	72.2	1703.5	517.6	25.1	58.8	-18.4	1364.1	-19.9	24.33	24.55	23.58
443.1	75.7	1737.4	556.8	25.6	61.6	-18.7	1385.7	-20.2	24.34	24.57	23.57
472.8	79.7	1735.3	588.2	24.4	65.4	-17.9	1397.6	-19.4	24.28	24.50	23.54
509.8	83.7	1704.9	610.7	19.7	71.2	-14.9	1425.7	-16.3	24.16	24.35	23.56
546.0	87.8	1692.2	640.1	17.2	76.2	-13.2	1445.4	-14.5	24.08	24.24	23.55
579.4	90.9	1704.2	670.3	15.6	79.9	-12.1	1475.0	-13.4	24.07	24.22	23.58
618.3	95.0	1731.1	716.0	15.7	83.5	-12.1	1496.8	-13.5	24.07	24.22	23.58
655.3	99.2	1798.3	782.4	19.3	84.9	-14.3	1508.4	-16.1	24.15	24.33	23.55
692.4	103.1	1815.6	826.1	19.3	88.4	-14.2	1523.8	-16.0	24.14	24.32	23.54
721.9	106.7	1826.3	864.6	19.7	91.3	-14.4	1527.1	-16.3	24.12	24.30	23.51
750.6	110.0	1836.7	901.1	20.0	93.9	-14.5	1532.2	-16.5	24.11	24.29	23.48
775.5	112.6	1844.2	930.4	19.9	96.3	-14.4	1539.5	-16.5	24.09	24.28	23.47
789.4	115.0	1850.4	956.4	21.1	97.5	-15.1	1529.6	-17.3	24.08	24.27	23.45

4. CALIBRATION PROCEDURE

4.1 Pressure measuring equipment

The pressure measured by a piezo-electric sensor is calculated from

$$P = \Delta x \cdot K \cdot \frac{kC_p}{\sigma}$$

where p is the pressure (atm)
 K is the overall oscilloscope sensitivity (volts/mm)
 Δx is the oscilloscope deflection measured on the photograph (mm)
 kC_p is the amplification factor (pC/V)
 σ is the transducer sensitivity (pC/atm)

The calibration curves of the pressure transducers used and from which the value of σ is obtained were supplied by the manufacturer. The curves were checked using a Kistler press^x (Kias Swiss type 6901 SN 56679). The transducer to be calibrated and a Kistler high precision reference transducer are mounted on the press through similar adaptors. The outputs of the two transducers are monitored as the percentage difference between them. The output of the reference gauge is monitored on a digital voltmeter. The sensitivity obtained by this method as compared to the maker's calibration of the two VKI transducers is shown in Fig. 8.

^x This was carried out at the Fabrique Nationale, Herstal, Belgium

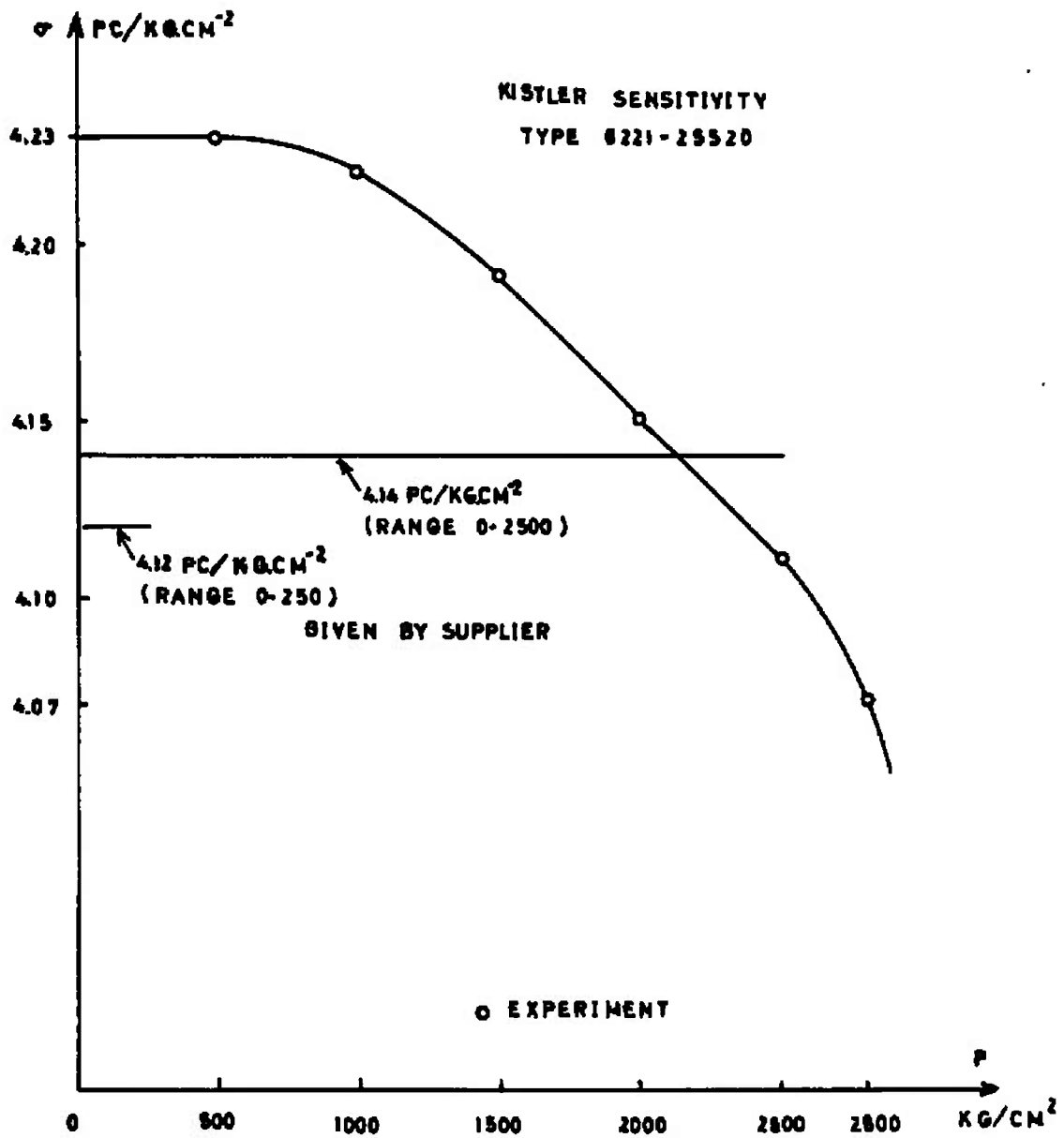


FIG. 8 Kistler pressure transducer calibration.

The performance of the charge amplifiers used in the compression tube was also checked out using the press combined with two calibrated VKI gauges and a calibrated charge amplifier supplied by FN. A fixed value of the amplification factor is initially set on the charge amplifier. As the pressure on the transducers was increased, the output voltage from the charge amplifier under calibration is monitored on a digital voltmeter, and the pressure is assessed from the instrumentation chain involving a calibrated transducer and the calibrated charge amplifier. Knowing the pressure, transducer sensitivity and the voltage, the correct value of $k C_p$ can be obtained for comparison with the amplifier setting. The percentage error for two values of $k C_p$ used in the compression tube experiments is shown in Fig.9.

It is seen that in both the transducer and charge amplifier calibrations, errors of the order of $\pm 1\%$ would be incurred if the makers calibrations were used. Corrections were made in the data reduction programs for these errors.

4.2 Lamp and optical system

The Philips D-8, 6 volt, 16-17 amp. rating tungsten ribbon lamp is calibrated against an optical pyrometer (of Evershed and Vignoles Ltd, London W4). For a black body filament temperature T_F at a lamp current I and voltage V , the effective brightness temperature T_{v_p} at a frequency ν_p is given by :

$$\frac{1}{T_{v_p}} = \frac{1}{T_F} - \frac{k}{h\nu_p} \ln \epsilon_T - \frac{k}{h\nu_p} \ln \tau_E - \frac{k}{h\nu_p} \ln \tau_R$$

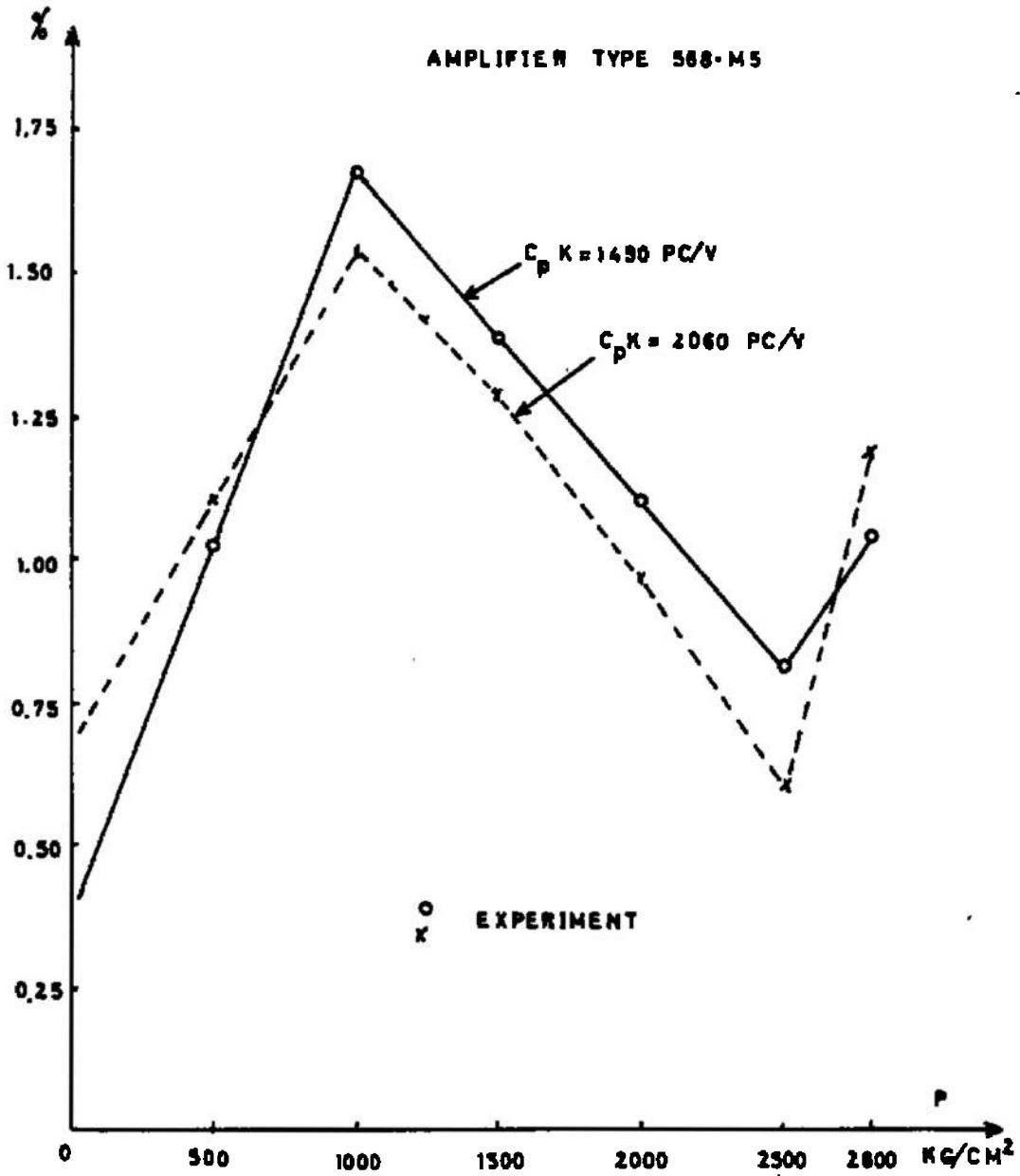


FIG. 9 Charge amplifier calibration curve.

where ϵ_T is the emissivity of tungsten at the frequency ν_p and is taken to be 0.43 (from tables)
 τ_E is the transmissivity of the glass envelope of the lamp
 τ_R is the transmissivity of the prism and lenses
 h is the Planck constant and
 k is the Boltzmann constant

The pyrometer measures the brightness temperature at a wavelength of 6650 Å, whilst the experiments are carried out at the sodium D-line wavelength of 5895 Å. It is assumed that there is a negligible error if τ_E , τ_R and ϵ_T are taken as constant for this wavelength change.

4.2.1 Estimation of transmissivity of the tungsten lamp glass envelope, τ_E

When just the lamp is viewed by the pyrometer then its reading $(T_{vp})_1$ is given by

$$\frac{1}{(T_{vp})_1} = \frac{1}{T_F} - \frac{k}{h\nu_p} \ln \tau_E - \frac{k}{h\nu_p} \ln \epsilon_T$$

If another similar lamp, but not illuminated is placed between the first lamp and the pyrometer, the light emitted from the tungsten ribbon crosses three thicknesses of glass. The new reading of the pyrometer $(T_{vp})_2$ is given by :

$$\frac{1}{(T_{vp})_2} = \frac{1}{T_F} - \frac{3k}{h\nu_p} \ln \tau_E - \frac{k}{h\nu_p} \ln \epsilon_T$$

The transmissivity of the envelope τ_E can be found from subtracting these two equations to give :

$$\tau_E = \exp \left[\frac{h\nu_P}{2k} \left(\frac{1}{(T_{\nu_P})_{P1}} - \frac{1}{(T_{\nu_P})_{P2}} \right) \right]$$

4.2.2 Estimation of transmissivity of the prisms and lenses, τ_R

This is estimated by viewing the radiating tungsten ribbon through the prism and lenses. The reading of the pyrometer $(T_{\nu_P})_3$ is given by :

$$\frac{1}{(T_{\nu_P})_3} = \frac{1}{T_F} - \frac{k}{h\nu_P} \ln \tau_E - \frac{k}{h\nu_P} \ln \epsilon_T - \frac{k}{h\nu_P} \ln \tau_R$$

which can be solved for τ_R

$$\tau_R = \exp \left[\frac{h\nu_P}{k} \left(\frac{1}{(T_{\nu_P})_{P1}} - \frac{1}{(T_{\nu_P})_{P3}} \right) \right]$$

Calibrations carried out show that both τ_E and τ_R vary with temperature as shown in Fig.10.

4.2.3 Estimation of the effective brightness temperature at a particular frequency

The temperature of the lamp at the centre of the sodium D-line frequency, ν , is given by

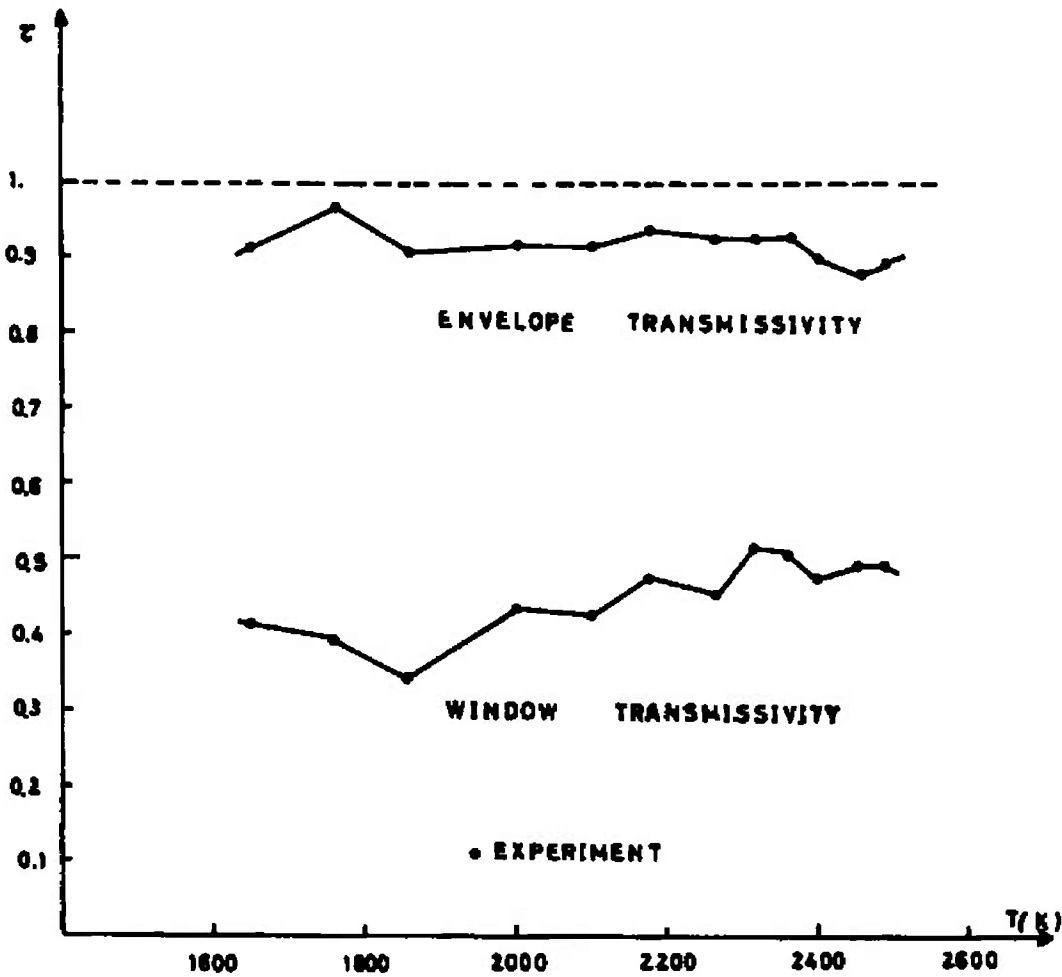


FIG. 10. Variation of glass transmissivity with temperature.

$$\frac{1}{T_v} = \frac{1}{T_F} - \frac{k}{h\nu} \ln \tau_E - \frac{k}{h\nu} \ln \epsilon_T - \frac{k}{h\nu} \ln \tau_R$$

The unknown T_F can be eliminated by subtraction from the previous equation to give :

$$\frac{1}{T_v} = \frac{1}{(T_{v_p})_3} - \frac{k}{h} \left(\frac{1}{\nu} - \frac{1}{\nu_p} \right) \ln \tau_E E_T \tau_R$$

The results of the calibration of the effective brightness temperature of the tungsten ribbon lamp used in the experiments at frequency ν as seen in the test section is presented in Fig.11.

The tungsten ribbon lamp is powered by a stabilized 6V 16A power supply. The 50 Hz ripple of light intensity due to mains supply is less than 3% during the tests and introduce an error of 0.5% on the measurement of gas temperature.

4.3 Recording equipment

4.3.1 Time bases

In these experiments the most important feature is to provide accurate synchronisation of the traces taken rather than knowledge of the absolute value of the time base. The method of synchronisation is carried out by injecting on one trace of each oscilloscope (pressure and piston motion traces) a signal from a 1 kHz square wave generator.

4.3.2 Amplitude sensitivity

The vertical sensitivity of the oscilloscopes was

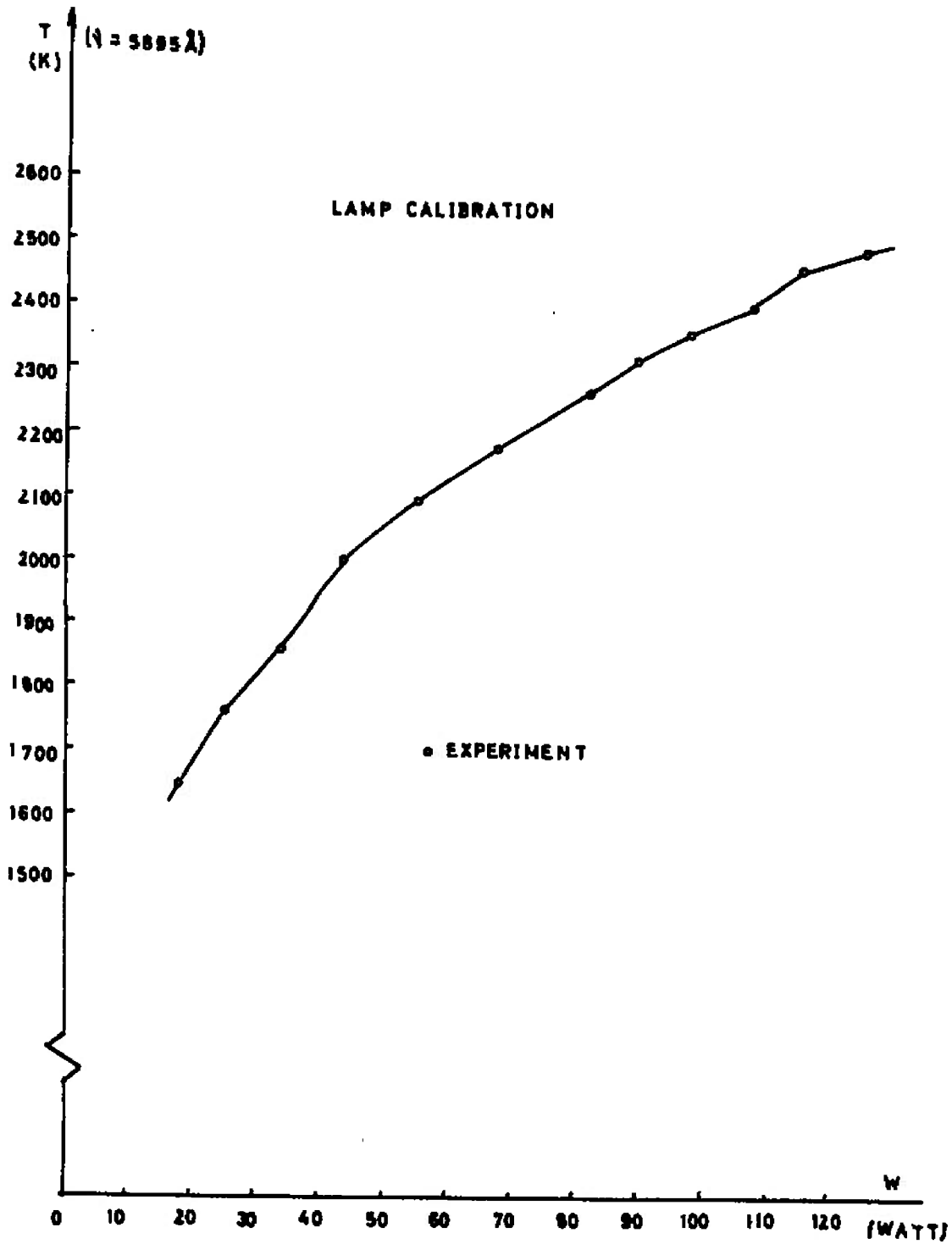


FIG. 11 Lamp calibration.

determined by injecting a calibrated square wave onto the beam of the scope which was photographed with the same polaroid camera as used in the experiments. Both experimental and calibration traces were read at the same position of a trace-reader constructed at the Institute which itself was checked for linearity and repeatability by measuring many times an accurate finely divided scale. The resolution of the measuring table is about 5 μm . A cross wire on the traveller allowed easy selection of the centre of the oscilloscope traces which were typically about 0.5 millimeters thick. Typical corrections of oscilloscope sensitivity from switch settings are of the order of 5%.

4.4 Photomultipliers

The EMI 9558C is excited by a "Fluke" Type M412B high voltage stabilized d.c. power supply providing a voltage range from 0 to 2.1 kV in steps of 0.1 kV. The system is very stable over short periods of time, and it is not necessary to calibrate the system, since seconds before each test, a signal from the calibrated light source is recorded on the oscilloscope. The measurements of temperature during the test rely on this signal as a reference.

4.5 Position measurements

Lewis et al (Ref.6) have described the tare tests carried out to ensure that the maximum output from the variable reluctance transducer is obtained when the centre of the transducer coincides with the centre of a tooth and the minimum with the centre of a groove. Measurements using an accurate travelling microscope showed that the grooves had been machined such that an accuracy of 0.2% over a span of 10 grooves was achieved. It is estimated that the crushed lead pin can be measured to within 0.1 mm.

5. DISCUSSION OF UNCERTAINTIES

5.1 Justification of using a "dynamic" experiment to measure thermodynamic state

Non-equilibrium behaviour

During the measurement area of interest, i.e. the last millisecond of the first compression, the pressure and density of the gas increase by an order of magnitude and the temperature is doubled (Fig.12). As mentioned in 2.3, calculations have shown that over the high density range of interest, the relaxation time of the internally excited energy modes of nitrogen and oxygen of the order of 0.1μsecs are two to three orders of magnitude faster than the rates involved in the compression process, and hence we can conclude that equilibrium is maintained throughout the tests and the errors arising due to this assumption are negligible.

Instrumentation frequency response

Instrumentation response provides another source of uncertainty. Provided that the variables to be measured vary in a smooth way as illustrated in Fig.12 then instrumentation with a frequency response of 1kHz or better would be able to follow the signals with the predicted rise times with negligible attenuation. All of the elements in the measurement chain have responses considerably better than 10 kHz. More critical for these experiments however is the lag time between signals. Although a lag of 10μsec (typically equivalent to a phase lag of 2°) in these experiments will cause only slight uncertainties near the peak pressure when the pressure variation with time is small, at half the peak pressure the error could be as large as 3%. Such overall lags can be accrued from the combination of response times from transducers, carrier amplifier, charge amplifier, oscilloscope amplifiers, etc. This suggests that

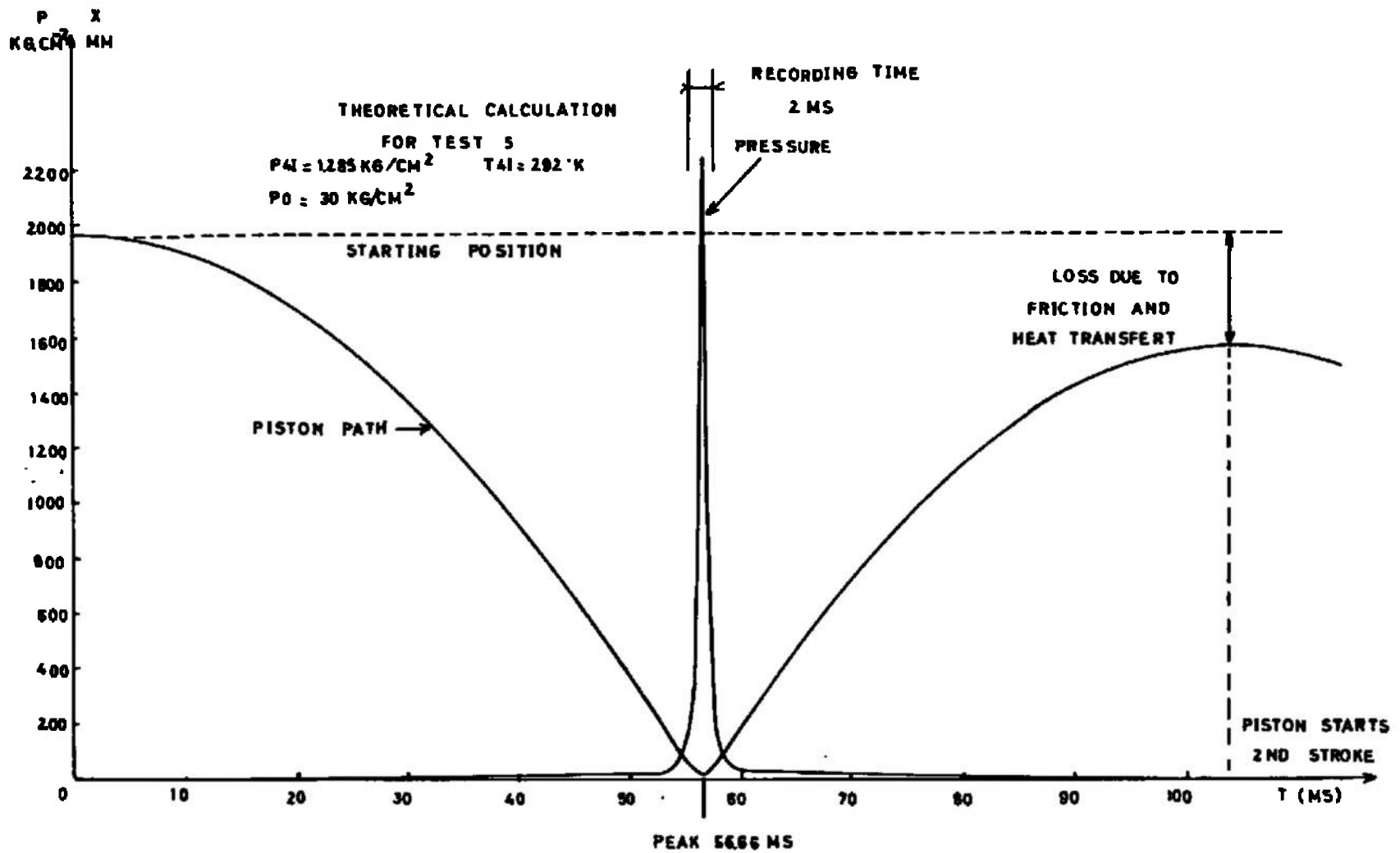


FIG. 12 Pressure variation during a test (theoretical).

only data near the peak is selected for study.

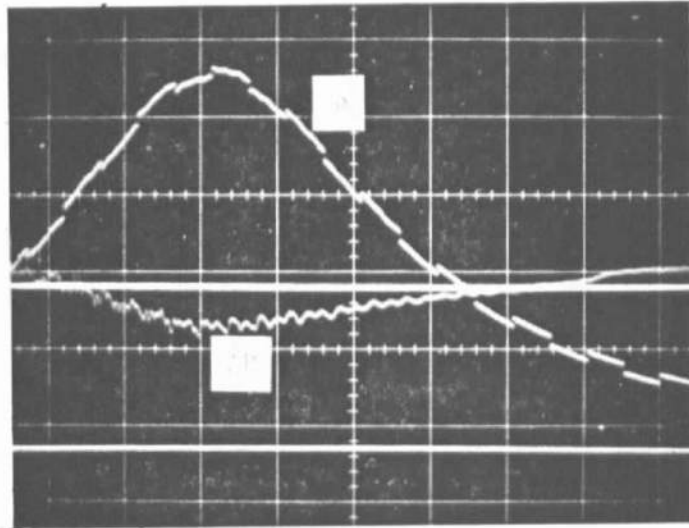
5.2 Pressure variations in the gas sample

A theoretical study was initially made to estimate the degree of uniformity in the volume of the gas sample. The compression cycle was calculated using the characteristics method to solve the unsteady one-dimensional flow problem. It was assumed that the gas was perfect. The results show that at the lower pressure cases pressure oscillations occur during the compression but disappear during the piston rebound. This is confirmed by experiments, however, these oscillations appear to be smaller than predicted (Fig.13)

5.3 Assessment of temperature variations in the gas sample

The results of the piston cycle calculation outlined above indicate that there are equivalent temperature variations through the gas sample. Since they are connected to the one-dimensional, unsteady flow pressure variations and these pressure variations were measured to be small, they themselves can be assumed to be small.

Another source of spatial temperature variation is that due to the thermal boundary layer on the cold tube wall. The simplified piston cycle program described in 3.1 was used to determine the extent of the thermal boundary layer and the total heat loss assuming that the heat losses were due to conduction. The boundary layer thickness was not greater than 0.02mm and the total heat loss was not greater than 3% of the total energy given to the sample by the piston. The losses are not important to the measurement since instantaneous



Sweep time $500 \mu\text{s}/\square$

P Scale $1\text{V}/\square$

ΔP Scale $0.2 \text{ v}/\square$

FIG. 13 Low pressure trace.

measurements of p, V and T are made during the last part of the test. The sodium line reversal technique can be affected by non-uniformities in temperature, since the temperature is averaged across the emitting and absorbing path. However, the non-uniformity is spread over only 0.4% of the light path, hence the errors due to this non-uniformity caused by conduction heat losses will not be expected to be greater than 0.4%

5.4 Experimental study of spatial uniformity of pressure in the test chamber

Two Kistler type 6221 piezo electric pressure transducers were placed in the end wall of the compression tube and in the sidewall respectively. The transducer in the end plate was flush-mounted to the surface. The transducer on the sidewall, had a passage of 52mm length and 2mm diameter leading to it. This latter position is the usual position of the transducer during the tests in which equation of state data is generated. Both outputs from the Kistler type 568M charge amplifier units which were adjusted to give nominally the same overall sensitivity were monitored on an oscilloscope as well as the difference between the outputs, but on a scale five times more sensitive. A series of experiments with this set up allowed an investigation to understand and help decrease experimental uncertainties, by making systematic changes and observing the results. Frequent calibrations with a Desgra gas and Huot deadweight tester up to 500 kg/cm² were made.

A typical trace from these experiments is also shown in Fig. 13. The output from the trace monitoring the pressure difference which reached a maximum difference of $\pm 2\%$ and occurred near the peak was possibly due to the following reasons :

1. Non-linearity of the pressure transducer output
2. Non-linearity of the charge amplifier output
3. Pneumatic lag due to the finite size of the passage to one of the transducers
4. Lag due to finite size of diaphragm thermal protection devices used in some of the tests
5. Thermal response of the transducer
6. Frequency response of the transducer.

The first two considerations if dominant would tend to cause deviations symmetrical with the pressure peak. The third consideration would tend to cause a deviation antisymmetric to the pressure peak. The final three considerations would tend to cause asymmetric responses but which would approximately cancel out if it is assumed the irregularities are similar in each case.

The level of difference and the symmetry of the pressure difference trace shown in Fig.13 tends to indicate that non-linearity of the transducers and charge amplifiers appears to be the chief cause of the difference. Corrections for non-linearity as determined by the calibration described in section 4.1 were hence included in the data reduction of the equation of state tests. Also it provides evidence to the calculations of section 5.2 which indicate that the finite passage length to the transducer causes negligibly small pneumatic lag.

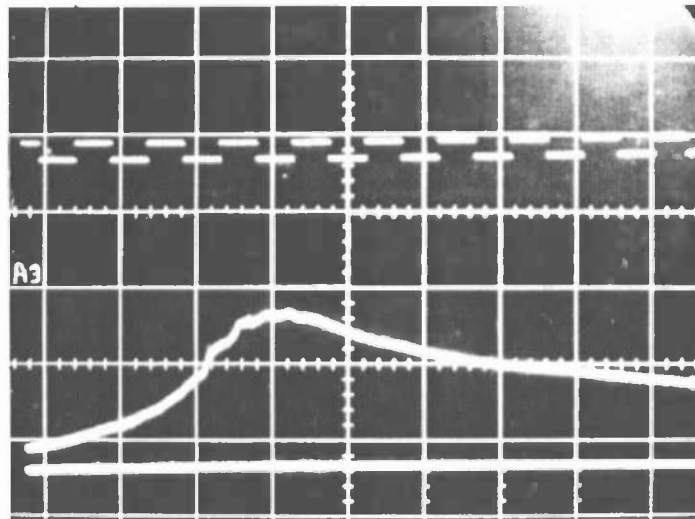
Other conclusions obtained from similar tests are :

i) Thermal protection of the transducer diaphragm prevents small errors (less than 1%). There is also no apparent lag or decrease in frequency response by placing a thin asbestos pad on the diaphragm to protect it from the hot gas. Hence it was decided to mount asbestos pad during the experiments.

- ii) The response of the gauge to vibrations is negligibly small
- iii) The overall frequency response of the measuring channels is fast enough to cause only small errors.

5.5. Experimental assessment of wall heat transfer during a test

A study has been made into the experimental uncertainties of the method of generation and measurement of the test slug associated with heat transfer and thermal effects. Measurements of the heat transfer rate have been accomplished using fast response thin film platinum resistance gauges mounted in the end wall. Many developmental difficulties were encountered in taking such a measurement in these gas conditions of high pressure and high temperature and high wall heat transfer rates. Pressure sensitivity of the output of the gauges (seen in early tests but using a different design of gauge) and vibration sensitivity were measured to be negligible by mounting the sensor in the compression tube, allowing it to be subjected to pressure loads and insulating it from heat loads. This was accomplished in one test by packing its surface with a 1mm thick layer of vacuum grease and in another test by protecting the sensor with oil trapped in a tube between the sensor and a close fitting but freely moving piston. A typical trace of the direct output of the gauge is shown in Fig. 14. The heat transfer rate variation was calculated from this surface temperature trace using a numerical solution similar to that given in Ref. 19. The value of heat transfer rate thus measured is a factor of 2 times that predicted by the theory of Knöös (Ref. 16) as described in Section 3.1 which takes into account heat losses only by conduction. Such a phenomenon could be caused by forced convection of the flow of gas caused by mixing. This mixing is thought to be caused by a ring-vortex type of motion



Sweep time $500 \mu\text{s}/\square$

T Scale $20 \text{ mv}/\square$

FIG. 14 Trace of thin film platinum gauge temperature.

caused by the oncoming piston (Ref.20), a flow configuration for which it is difficult to predict the heat transfer rate. This high value of measured heat transfer rate provides an important step towards explaining the temperature decays that occur in intermittent facilities of the order of 8°K per millisecond at 2000°K .

5.6 Gas leakages

Three circumferential nylon flexible seals are incorporated on the piston to prevent gas leakages (see Fig.3). One of the seals is placed on the rear of the piston to prevent driver gas from leaking and hence contaminating the test gas during the piston acceleration phase. The other two seals are placed in tandem close to the front of the piston to prevent the leakage of gas during the piston deceleration phase. The seals are designed to expose little of their surface to the test gas. O-ring seals are used everywhere else to prevent leaks from the compression tube. The seals were tested statically by loading the tube with 30 kg/cm^2 on one face of the piston and a vacuum on the other face. Only small losses were produced in times of several hours on both faces of the piston. A check of the dynamic effectiveness of the seals was seen when a pressure transducer was placed in the tube wall in such a position that the piston passed it during a test. A zero pressure was recorded when the transducer was located between the fore and aft seals.

5.7 Contamination of the gas

5.7.1 Nitrogen

Dry nitrogen with a purity of $99.9\%^x$ was used as the test gas. The impurities are mainly residuals of oxygen,

^x supplied by Air Liquide

hydrogen and water vapour. To minimise further contaminants being introduced by the transfer of the gas from the bottle to the barrel, the filling procedure was carried out in the following way.

The tube is first cleared throughout with acetone. The barrel is then evacuated to the order of 1mmHg pressure and maintained at this condition for a few minutes to check for leaks. The barrel is then filled with nitrogen to a pressure of 2 kg/cm², and a further check for leaks carried out over a few minutes. The tube is then evacuated once more and the barrel finally filled to the desired initial pressure. A limited amount of contamination may occur during a test due to hot high pressure gases attacking the small exposed surface areas of the O-ring and plastic seals.

5.7.2 Air

Ambient air was used throughout these preliminary tests as the test gas. The use of air brought up a problem of contaminants from the seals. Slight carbon deposits were seen on the tube walls after high temperature tests, which are assumed to come from oxidation of the plastic seals by the oxygen in the air. Similar deposits were seen when testing helium at very high temperatures (Ref.21).

5.8 Initial temperature of the test gas

The initial temperature of the test gas is taken as the laboratory temperature. This temperature is stable over periods of a day but varies between 18°C and 28°C during the year. Corrections for this temperature to initial entropy

* supplied by Air Liquide

are made in the final data reduction. During the filling of the tube, the gas temperature is slightly lowered. Since several minutes elapse before the test is carried out, it is assumed that the gas temperature reaches that of the barrel.

5.9 Summary of measurement uncertainties

The following table summarises the results of the uncertainty study of the measurements at peak conditions presented in the earlier sub-sections.

Measurement	Remarks	Error
Pressure	Transducer and charge amplifier errors assumed small since directly calibrated. Oscilloscope calibration and trace reading.	- $\sim \pm 1.0\%$
Temperature	25°K error in pyrometer reading at 2,500°K 50 kHz ripple 3% at 2,500°K	$\sim \pm 1.0\%$ $\sim \pm 0.5\%$
Position	Trace reading 1% Groove machining Lead pin measurement } 0.3% Timing	$\sim \pm 0.2\%$ $\sim \pm 0.3\%$ $\sim \pm 1.0\%$
Synchronisation		$\sim \pm 0.5\%$

Overall error (as a sum of above) = 4.5%

Because, smaller deflections away from the peak conditions are measured, and furthermore synchronisation is more difficult, the sum of the overall errors is expected to be in the range of $\pm 7\%$ to 10% .

6. RESULTS AND DISCUSSION

6.1 Measurements in nitrogen

Table 3 summarises the region in which equations of state tests were carried out using nitrogen as the test gas. The initial conditions, and conditions defining the range over which pressure, density and temperature were measured are there presented. The peak pressure at the initial dimensionless entropy for each test are plotted on a Mollier chart in Fig.15 to illustrate the overall range of the tests and to aid identification of each individual test. All 14 of those tests in which satisfactorily readable oscilloscope traces of all three measured quantities are presented.

From the computer output of the data reduction programs (described in Section 3.2.2) are plotted p_{calc} against p_{meas} , ρ_{calc} against ρ_{meas} , T_{calc} against T_{meas} (Fig.16-18). The deviations between the measured and calculated quantities are plotted in Fig.19 against an arbitrary time. The dimensionless entropy calculated from each pair of the three measured quantities is plotted in Fig.20. All of the data from all fourteen runs has been reduced and plotted in the above manner but not included in the report. The tabulated and plotted results are held by VKI and a copy has been forwarded to AEDC.

The following discussion is based upon these plots :

a) In some tests the curves representing the compression and expansion can be seen to be not coincident, as one might expect. This is mainly due to errors in synchronisation of traces. The traces are synchronised with respect to the timing signal, but ignores lags in instrumentation, which are

TABLE 3 Summary of nitrogen tests.

NO	P4I	T4I	p4I	S4I/R	P(PEAK)	P(MIN)	T(PEAK)	T(MIN)	p(PEAK)	p(MIN)
5	1.285	292.15	1.159	22.792	2240	290	1960	1500	220	63
6	1.285	295.15	1.147	22.828	735	405	1600	1480	109	70
8	1.285	296.15	1.143	22.840	1060	300	1705	1400	137	62
10	1.000	285.15	0.892	23.080	1460	525	1930	1600	154	75
12	1.000	296.15	0.888	23.092	2520	550	2090	1650	208	83
13	1.000	296.15	0.889	23.082	3020	300	2320	1750	220	63
14	2.000	297.15	1.773	22.408	1950	700	1785	1450	204	106
15	2.000	298.15	1.767	22.420	1170	620	1570	1220	156	96
19	1.285	297.15	1.139	22.852	2920	530	2120	1400	233	86
20	2.000	297.15	1.773	22.408	2390	600	1830	1280	237	86
23	0.700	296.65	0.621	23.455	1960	300	2240	1630	163	52
24	1.000	296.85	0.887	23.101	2530	450	2130	1470	200	70
25	1.000	295.15	0.882	23.080	2720	340	2195	1650	211	65
26	2.000	295.15	1.785	22.384	1200	540	1550	1285	157	97

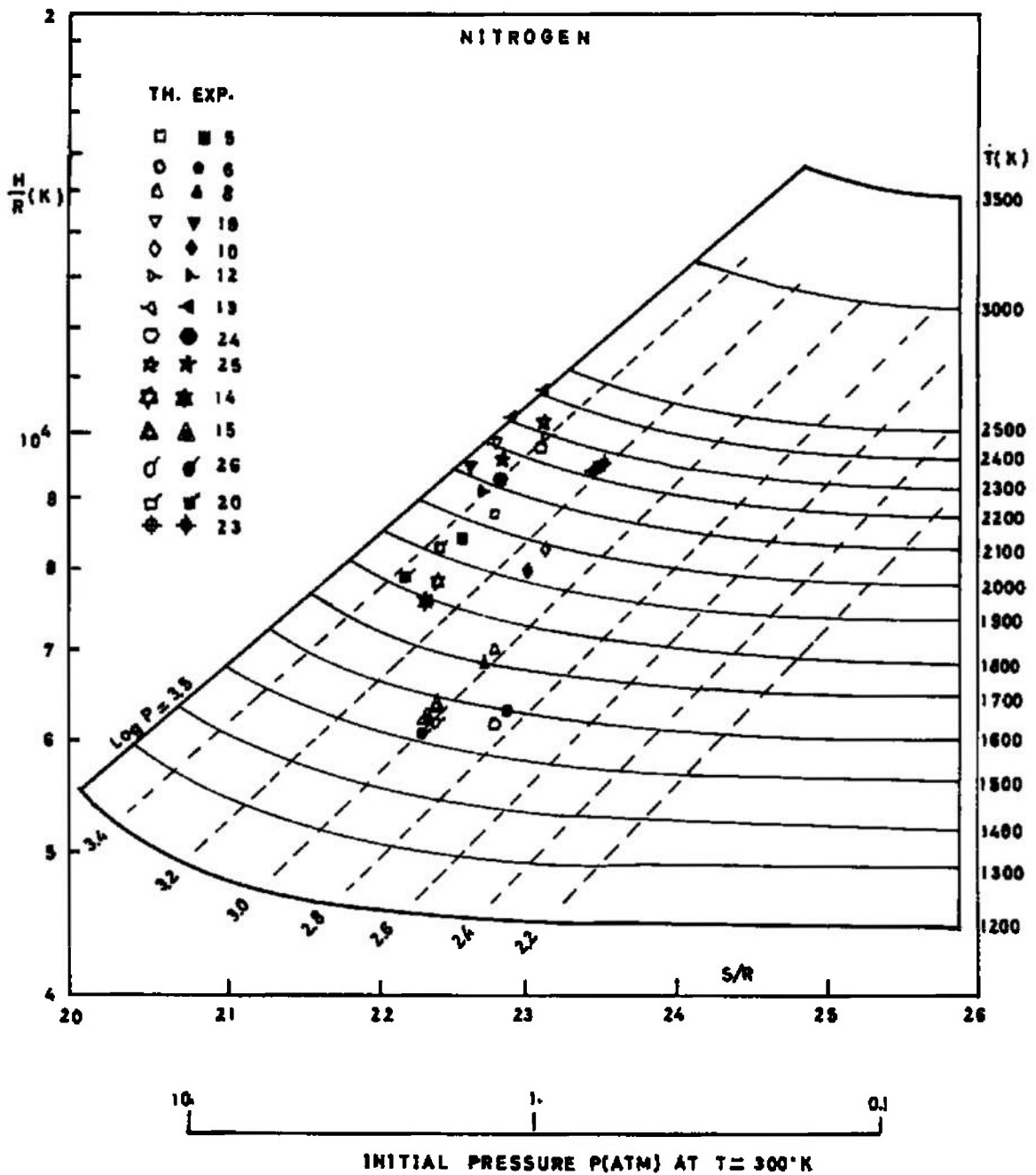


FIG. 15 Tests carried out with nitrogen(peak conditions).

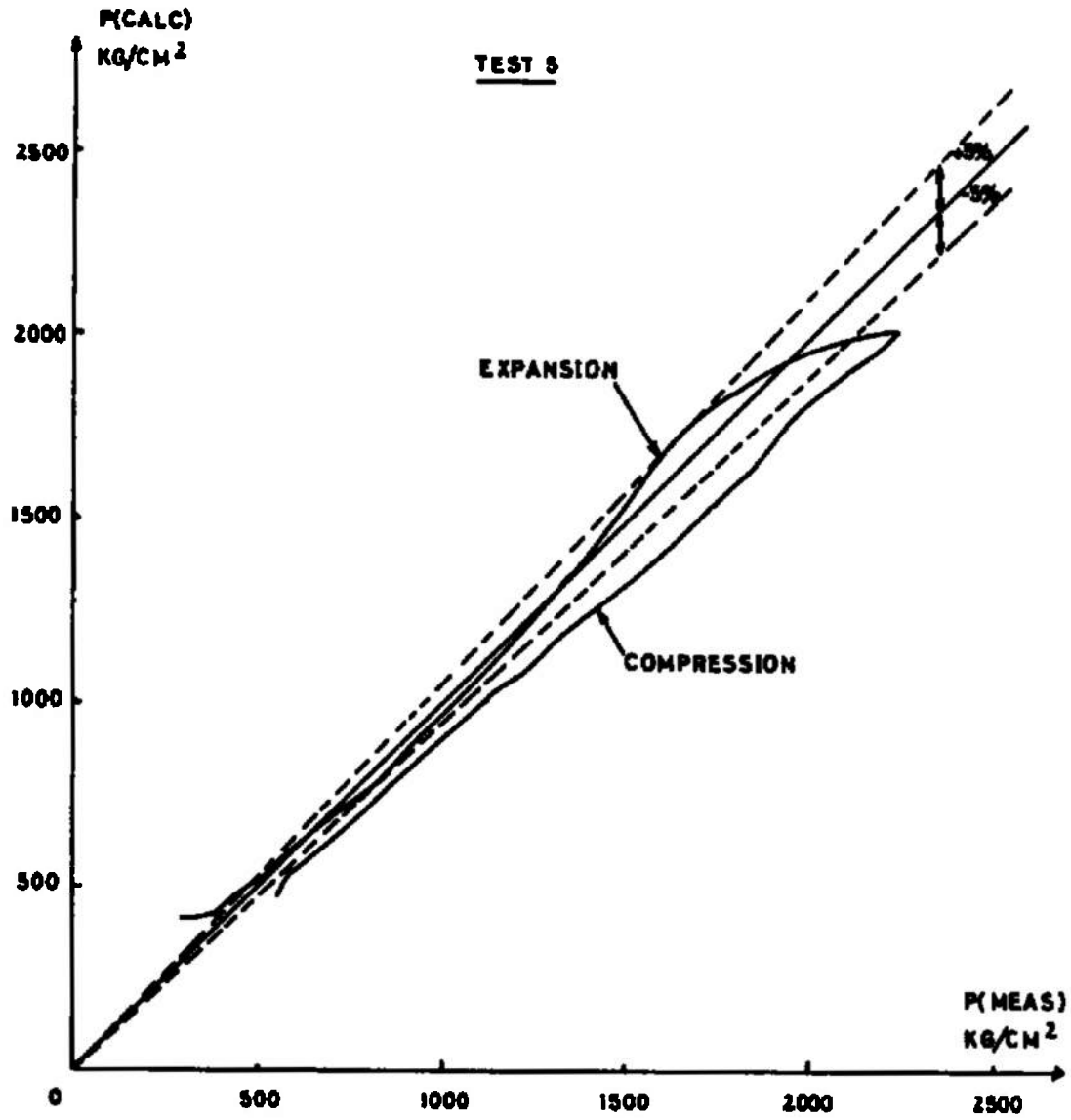


FIG. 16 P calculated against P measured in N₂.

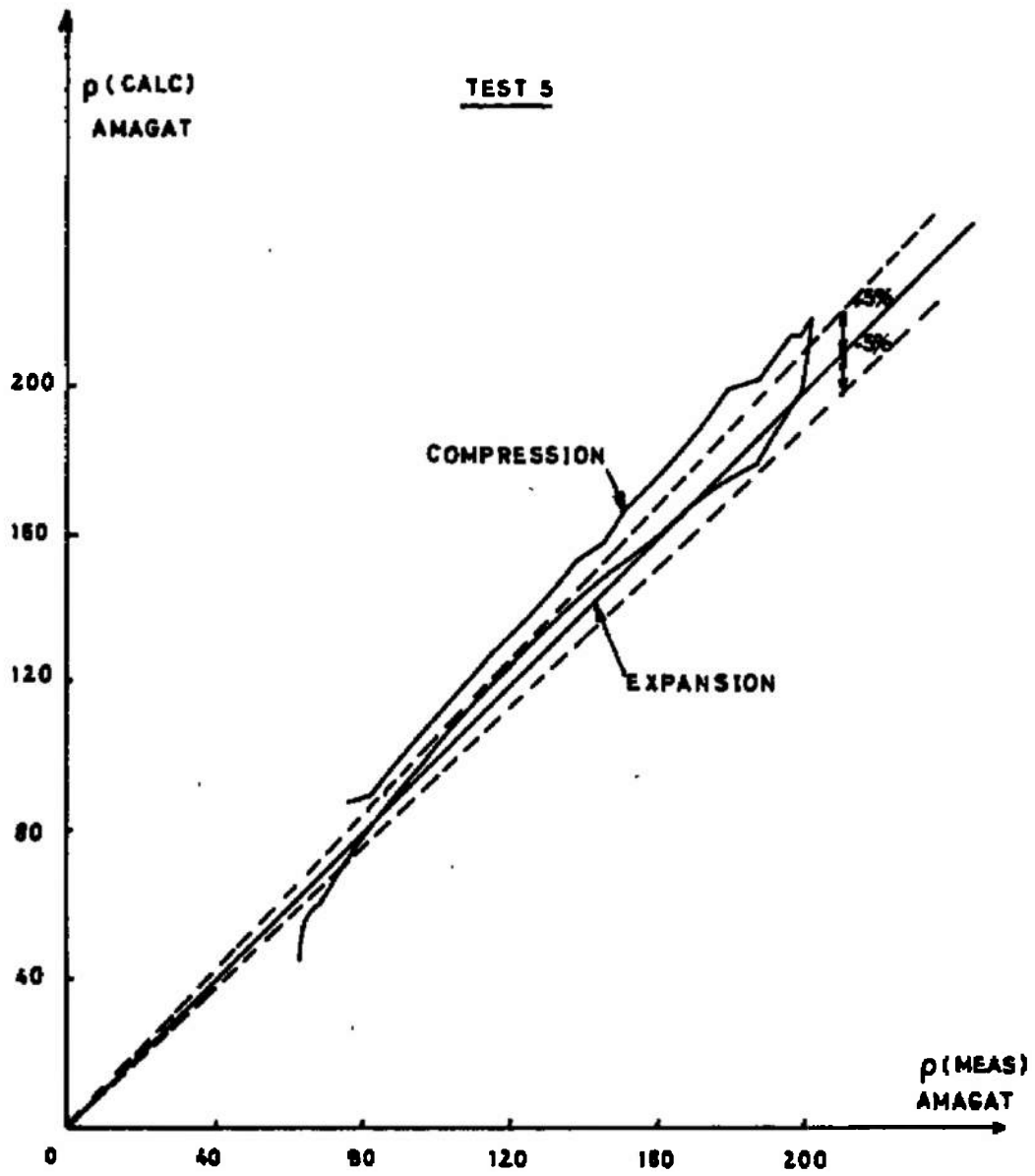
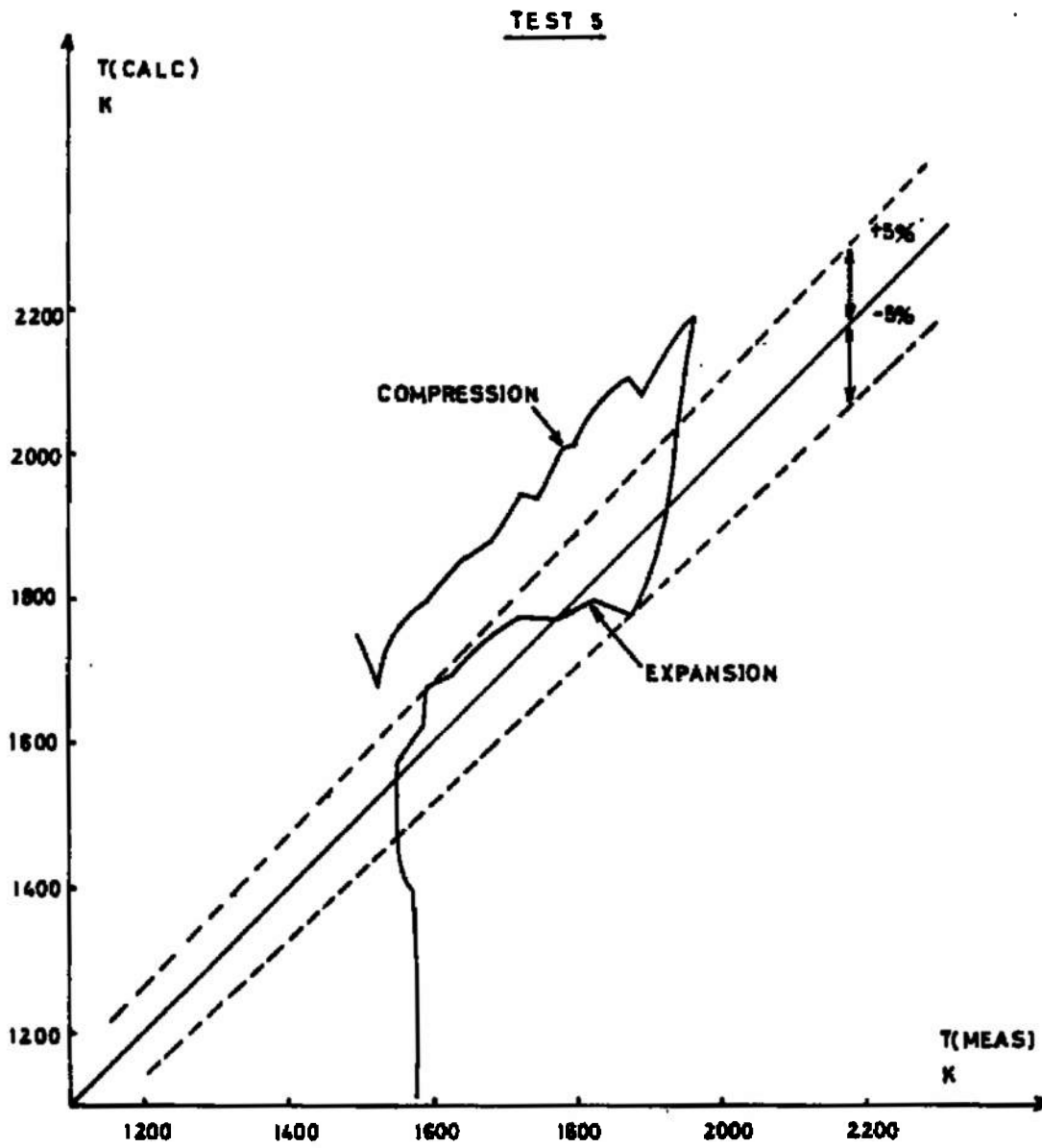


FIG. 17 ρ calculated against ρ measured in N_2 .

FIG. 18 T calculated against T measured in N_2 .

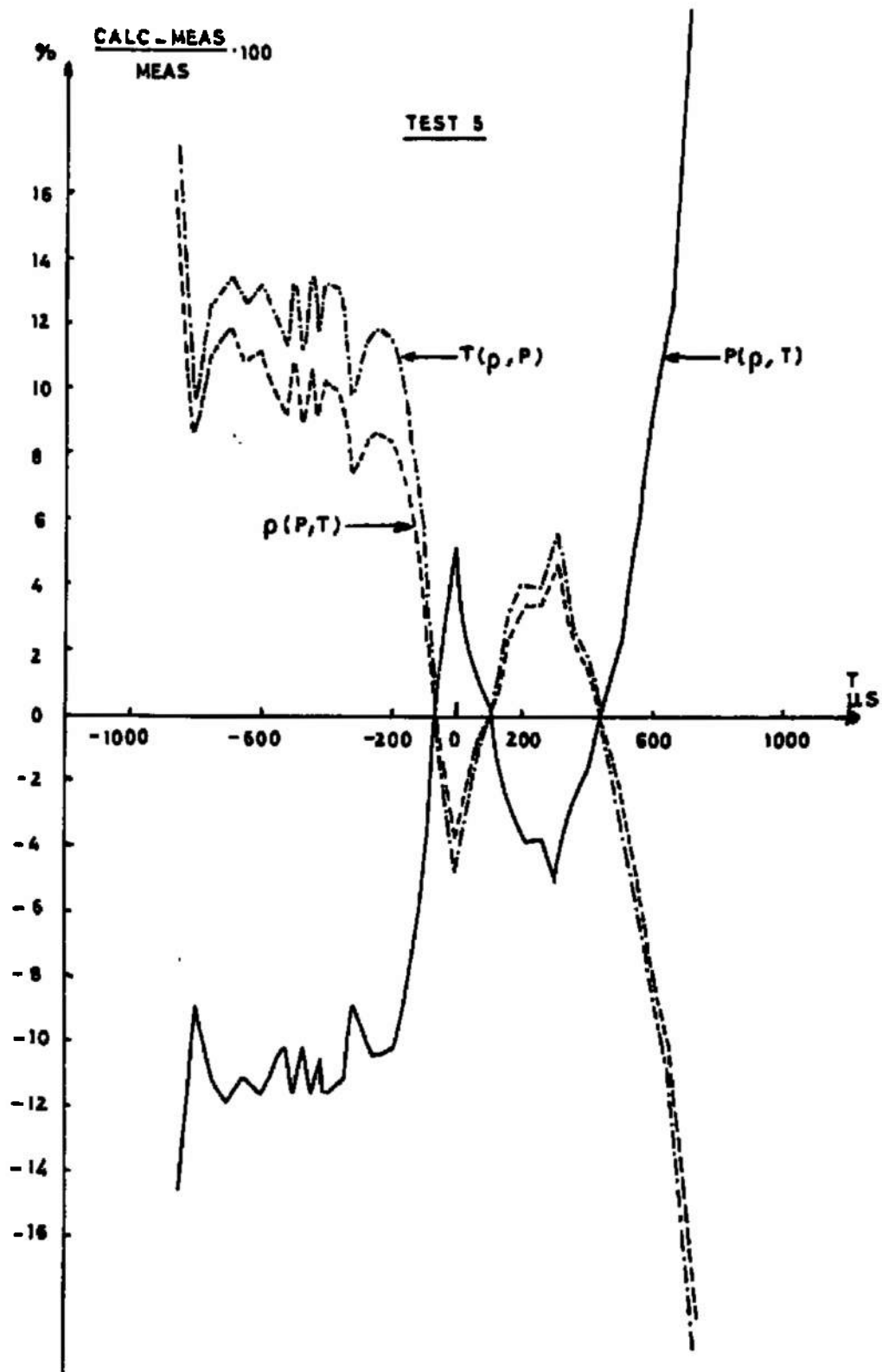


FIG. 19 Departures in % between equation of state on N₂ and experiments versus time (N₂).

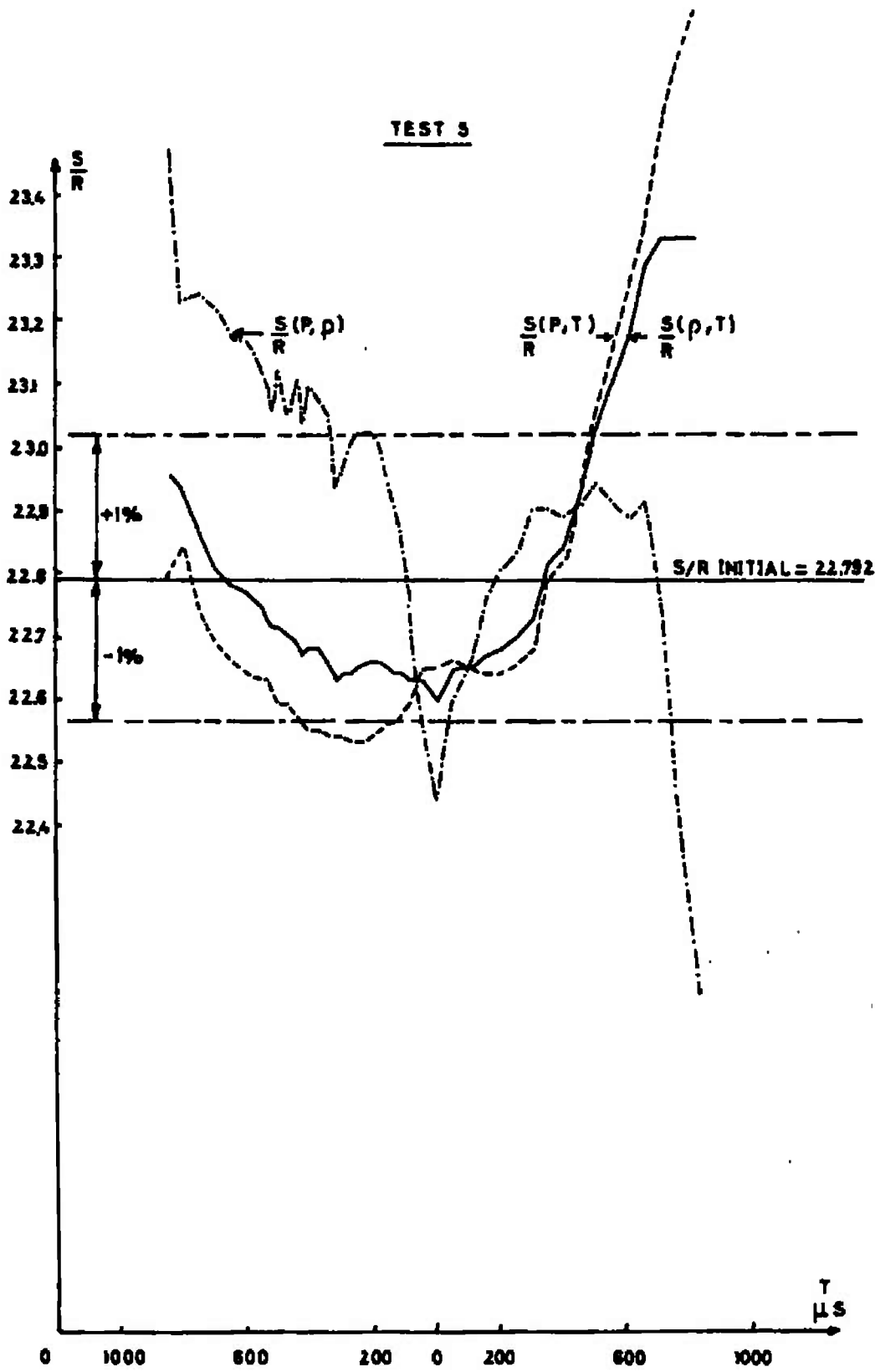


FIG. 20 Dimensionless entropy versus time (N_2).

difficult to predict to within the 10 μ sec accuracy necessary to keep the errors to small values. A better method of synchronising the signals is to assume that the parameters measured, i.e. p , ρ , T will reach peak conditions at the same time and to re-align the signals accordingly. This assumption can be made provided that the lags are not so large that the signal is not attenuated by any appreciable amount.

b) More scatter is obtained in the measurements of temperature than in the other two measurements. This measurement is the least straight forward of the techniques used. The sodium line reversal technique as applied to the present experiment gives accurate measurement in a narrow region when the gas temperature is close to and below the lamp temperature selected. Errors then get exponentially larger at lower gas temperatures. Furthermore the chopping frequency limits the time resolution of the curves of emission and absorption. An interpolation has to be made between the chopped traces.

c) Some of the pressure traces from the low pressure tests show small oscillatory deviations from the expected smooth variation. A calculation of the compression cycle using a characteristic solution for the unsteady one-dimensional flow in front of the piston have shown that oscillations in both pressure and temperature (see Sections 5.2 and 5.4) exist. These are not easily seen in the temperature traces since the light chopping is nearly in phase with them. These pressure oscillations were smoothed out when taking the deflections from the traces.

d) There is found an asymmetry about the peak value in the results of temperature which is as yet not fully explainable. This appears to arise from the distinct asymmetry of the light absorption measurement as illustrated in Fig.5. The absorption is seen to be greater on the expansion part of the cycle than

on the compression part. The emission measurement however is always symmetrical about the peak as expected. The final temperature is not greatly affected by the absorption term in Equation 1 (Section 2.3), however, it is felt that in view of the small errors introduced more weight should be given to compression data rather than expansion data. The following possible reasons are given for this asymmetry.

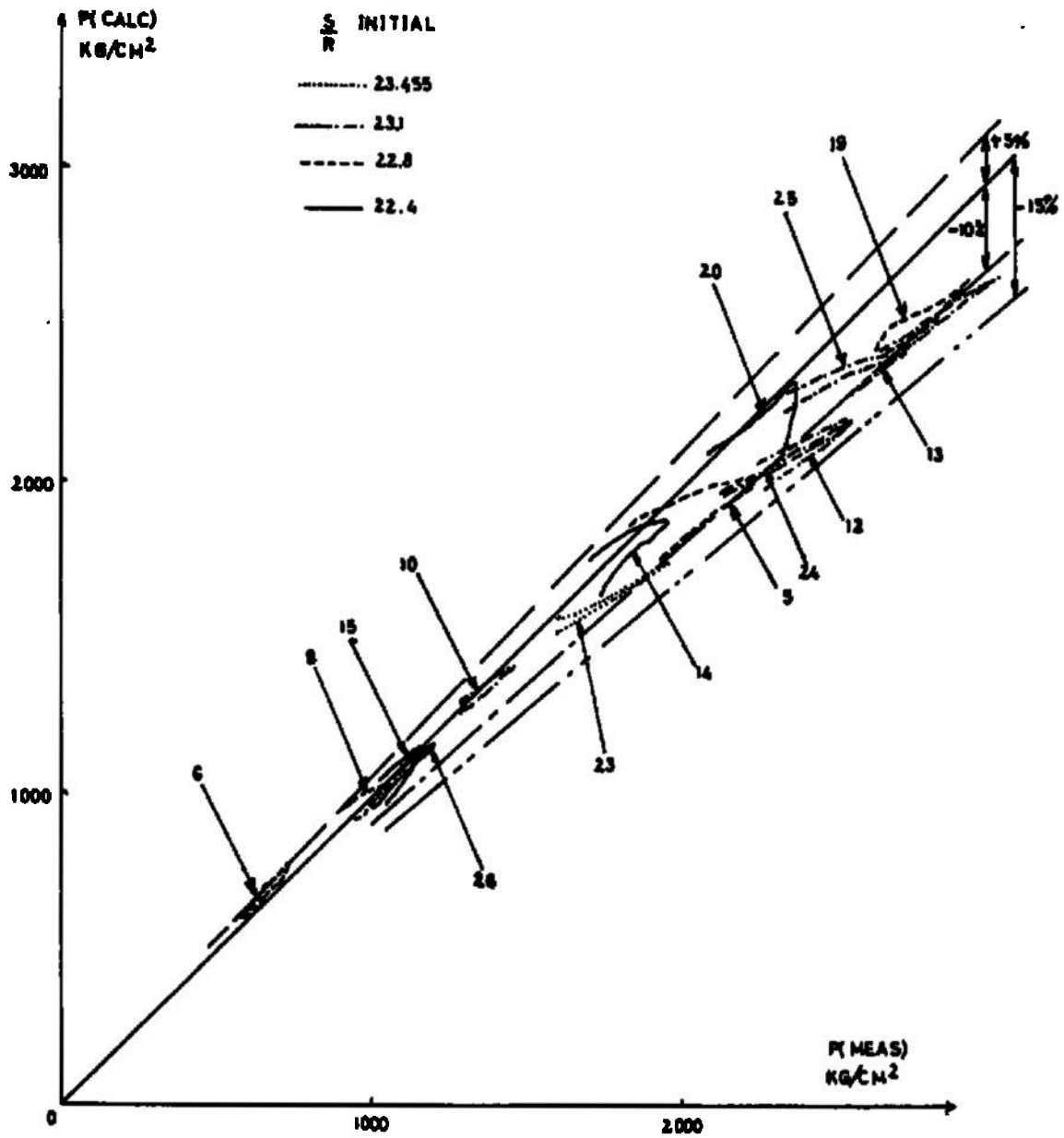
i) The optical system may have been sensitive to the vibration due to the recoil of the facility. Such sensitivity was found to be absent by examining the temperature traces when the observation cavity was isolated from the test chamber. There was no discernible response to the signal from the chopped light beam showing that the measuring system was vibration insensitive.

ii) The gas may become more opaque to light the denser it is, and the more turbulent the state of the gas. The latter is expected to be true during the latter stages of the cycle, hence the absorption by this process may be more important than in the earlier stages. A test was carried out after paying particular attention to the cleaning of tube surfaces and without introducing the sodium seed but no conclusion could be made from the results of the test since even the smallest residual traces of sodium appear to remain emitting and absorbing, and a thus similar asymmetrical absorption trace was obtained.

iii) The extra absorption in the expansion part of the cycle may be caused by slight contamination from the sodium azide, ablated plastic and other sources.

It was not possible to give any conclusion regarding this uncertainty on consideration of the results of the test described earlier.

The data obtained from the fourteen runs is reviewed by plotting all the data in Figures 21 and 22. In the former Figure, P_{calc} has been plotted against P_{meas} and the latter,

NITROGENFIG. 21 Summary of P calculated against P measured in N₂.

NITROGEN

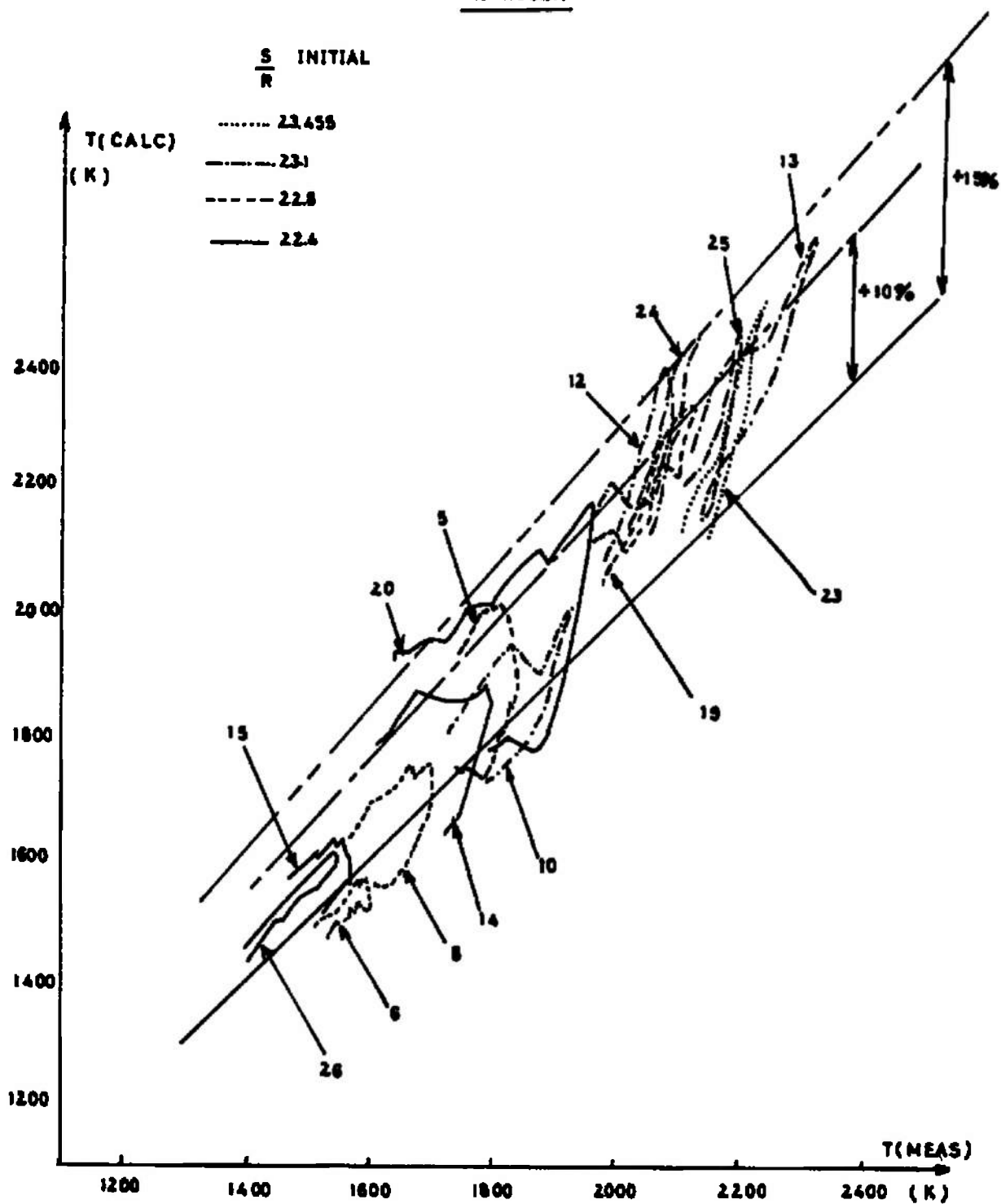


FIG. 22 Summary of T calculated against T measured in N₂.

T_{calc} against T_{meas} . Figure 21 illustrates that there is good agreement between measurement and calculation at pressures below 1400 Kg/cm², but a gradual trend for the measured pressure to be above that calculated at higher pressures. There is a discernable trend with entropy in that the deviation is slightly more marked for the higher entropy cases than the lower entropy cases. Figure 22 illustrates that measured temperature gives good agreement with calculated temperature below 1700°K, and a trend for the measured temperature to lie below the calculated values at high temperatures. In this latter case, there appears to be no trend with different entropy cases.

The result outlined in this last paragraph illustrates that the equation of state used is predicting the measurements in the region of $P > 1600$ Kg/cm² and $T > 1700$ °K only to within 10 - 15%. It is noted that this particular region gives the largest deviations between the AEDC tables for N₂ (Ref.18) and the Enkenhus-Culotta equation of state (Ref.4). However, no improvement in agreement is obtained by using the former theoretical equation of state data presented in the AEDC tables.

6.2 Measurement in air

The data from the 12 tests carried out in air have been presented in the same way as for nitrogen in Table 4 and Figures 23 to 30. In the review graphs (Figs 29 and 30), the reverse trend of deviation between measured and calculated values is found with air than in nitrogen but the magnitude of the deviation is considerably higher ranging between 10% and 40%.

TABLE 4 Summary of air tests.

NO	P41	T41	ρ 41	S41/R	P(PEAK)	P(MIN)	T(PEAK)	T(MIN)	ρ (PEAK)	ρ (MIN)
38	0.952	295.15	0.85	23.951	1498	344	2052	1746	200	37
39	0.952	295.15	0.85	23.951	790	225	1850	1480	120	37
40	0.952	296.15	0.84	23.961	727	390	1830	1485	109	37
41	0.952	297.15	0.84	23.971	857	320	2130	1660	135	37
42	0.58	297.95	0.51	24.476	420	220	1870	1590	63	22
44	0.58	299.15	0.51	24.488	680	240	1980	1605	98	22
45	0.58	299.35	0.51	24.490	1060	240	2110	1770	144	22
46	0.58	300.15	0.51	24.498	1430	390	2250	1680	220	22
48	0.58	297.75	0.51	24.473	1360	203	2260	1790	175	22
50	0.952	296.85	0.84	23.968	1295	417	2285	1770	203	37
51	0.952	296.95	0.84	23.968	2505	433	2170	1821	348	37
56	0.952	295.35	0.85	23.953	1967	490	2180	1710	266	37

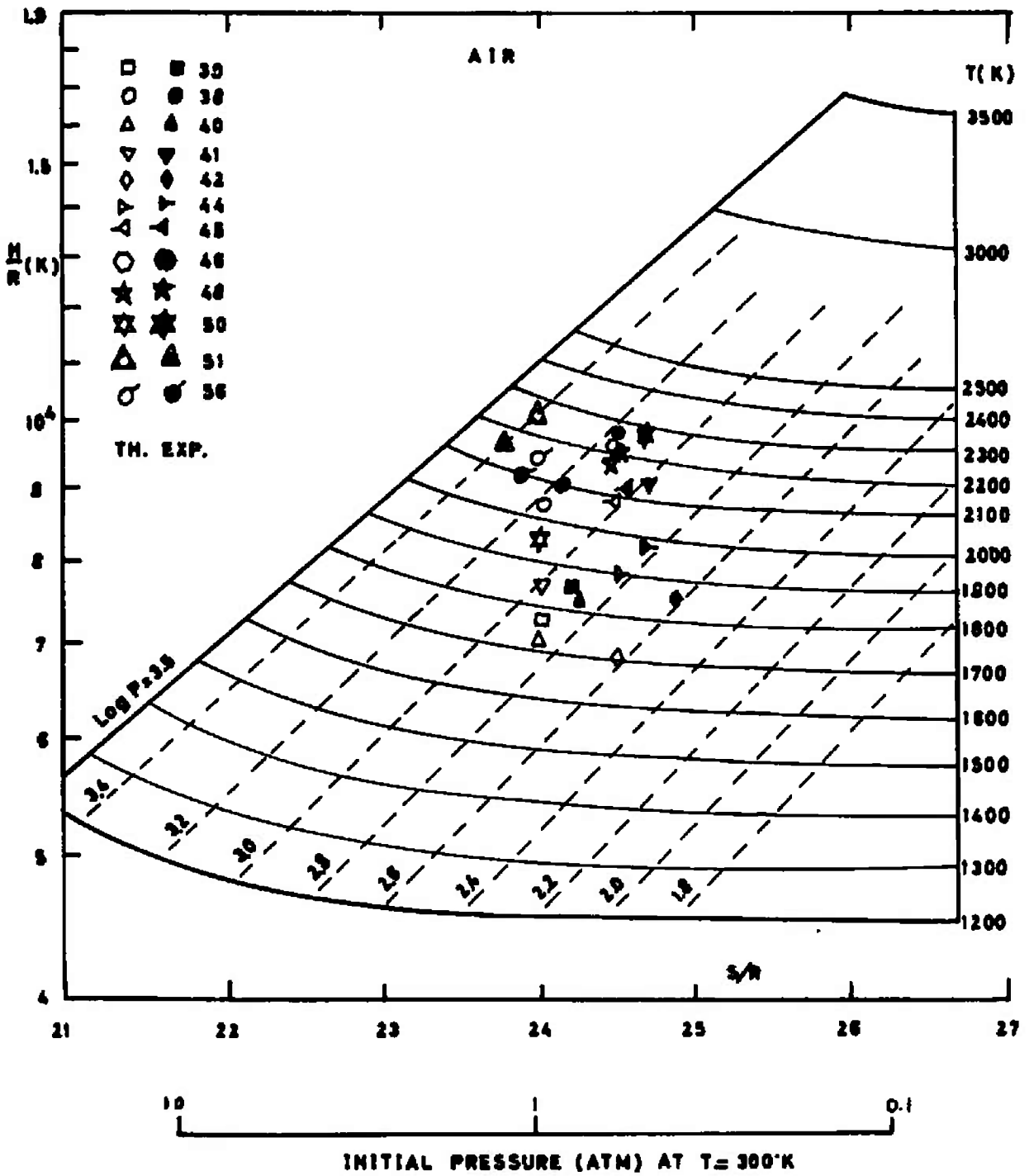


FIG. 23 Tests carried out with air.

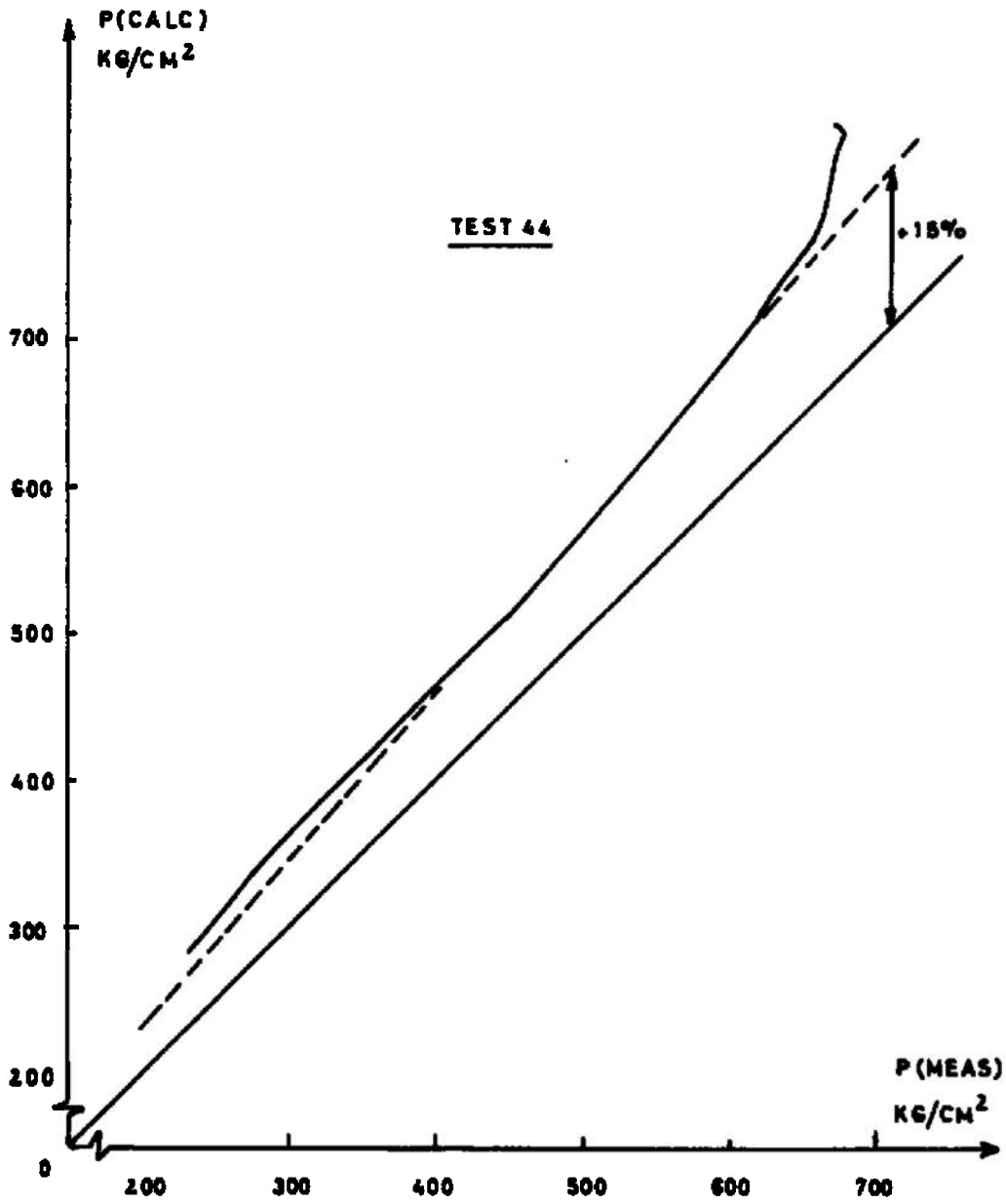


FIG. 24 P calculated against P measured in air.

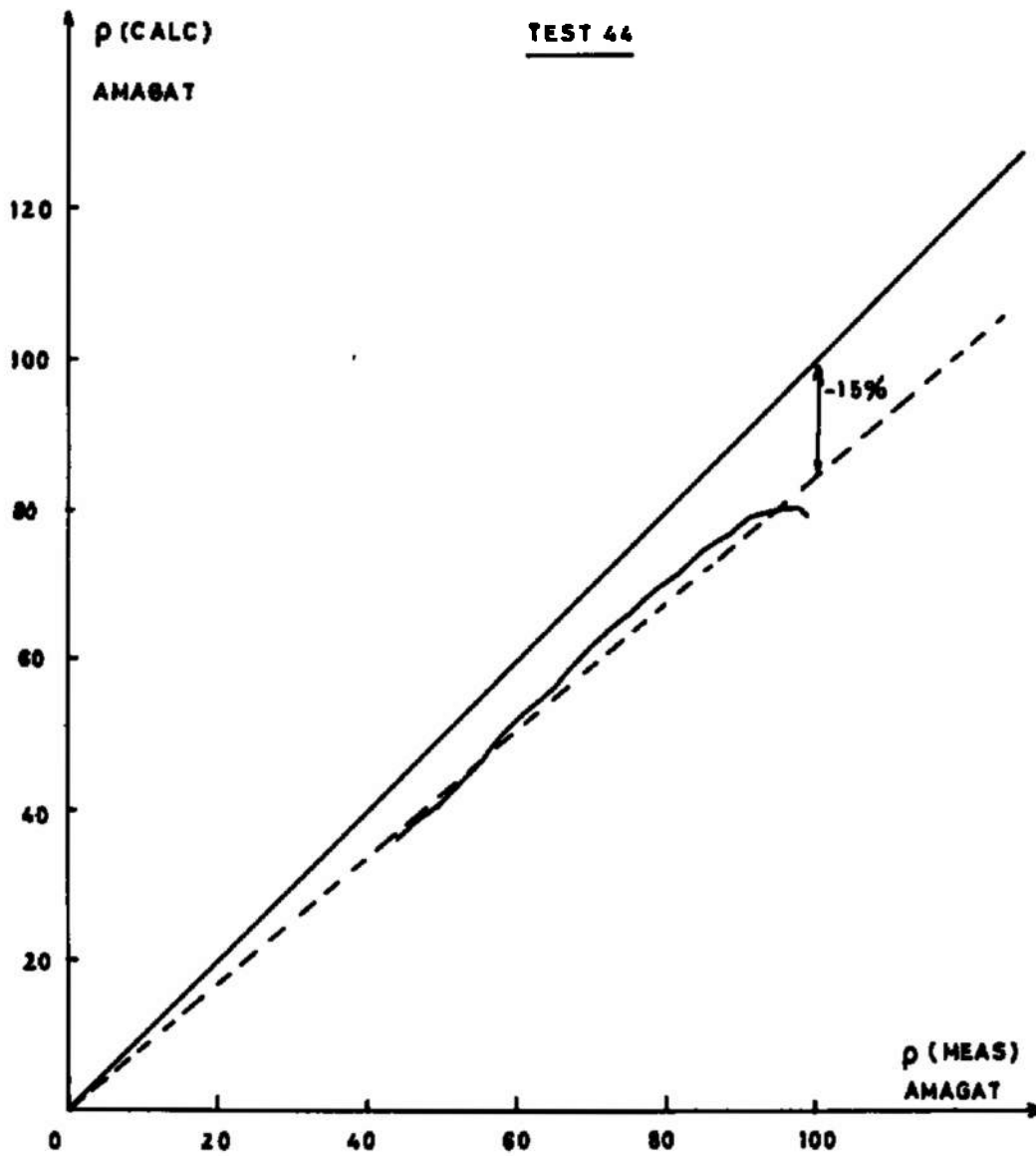


FIG. 25 ρ calculated against ρ measured in air.

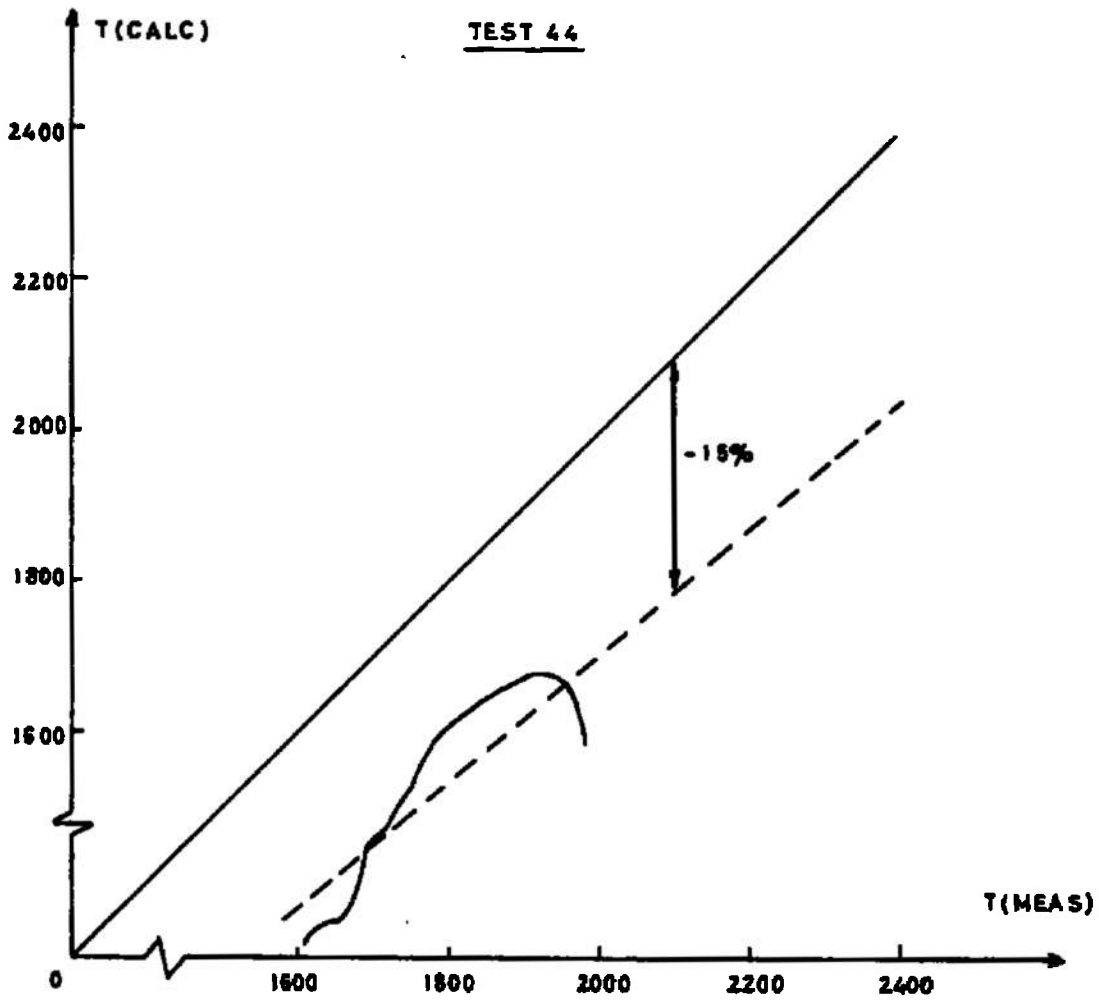


FIG. 26 T calculated against T measured in air.

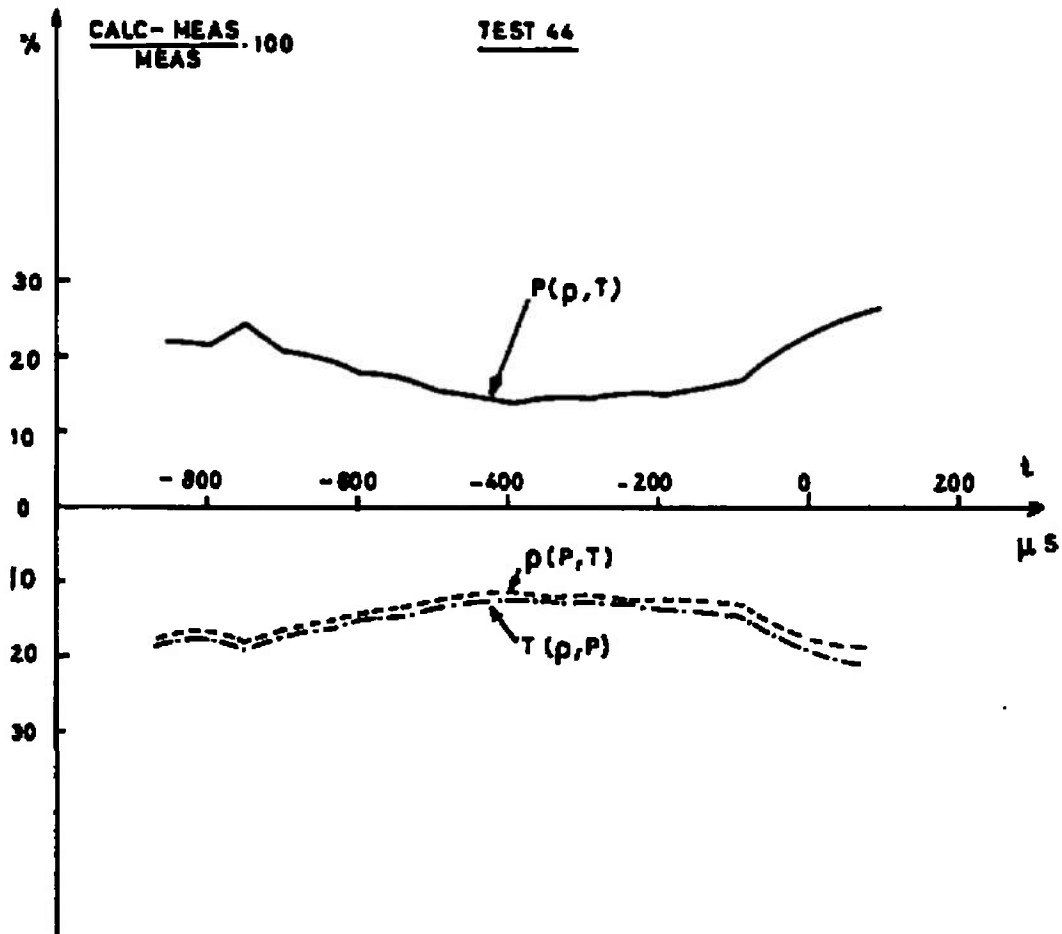


FIG. 27 Departures in % between tables of air and experiments versus time.

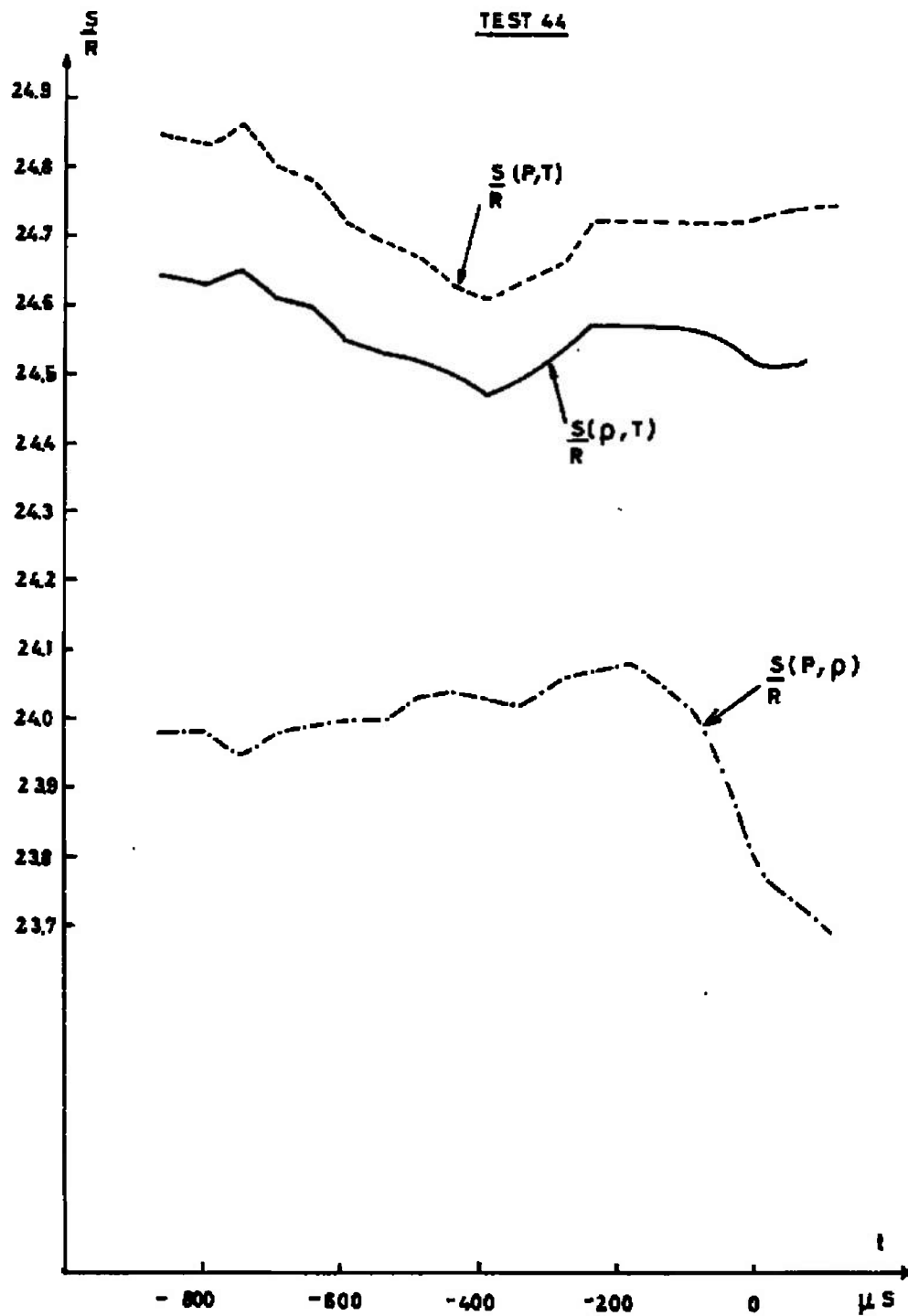


FIG. 28 Dimensionless entropy versus time (Air).

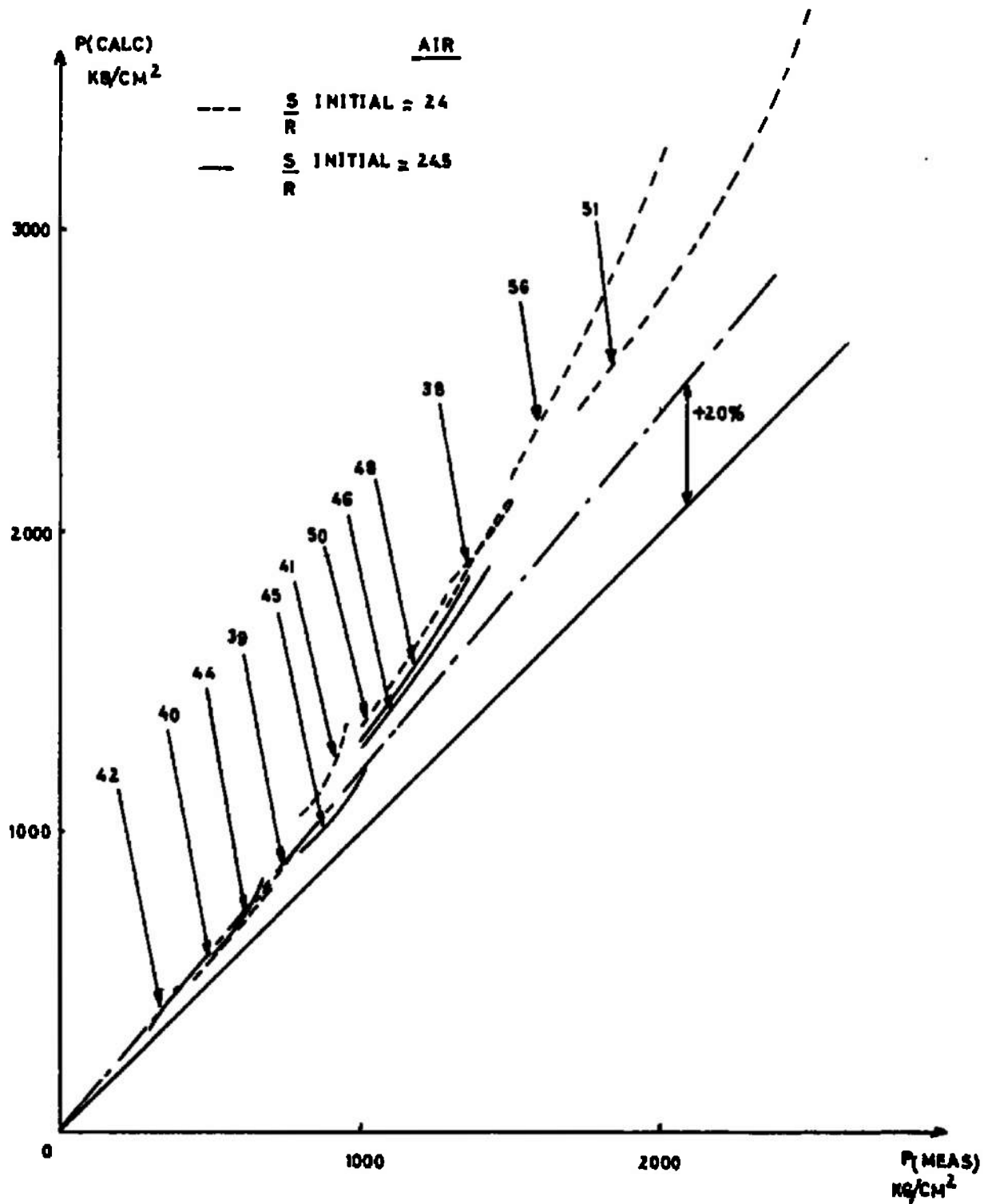


FIG. 29 Summary of P calculated against P measured in air.

AIR

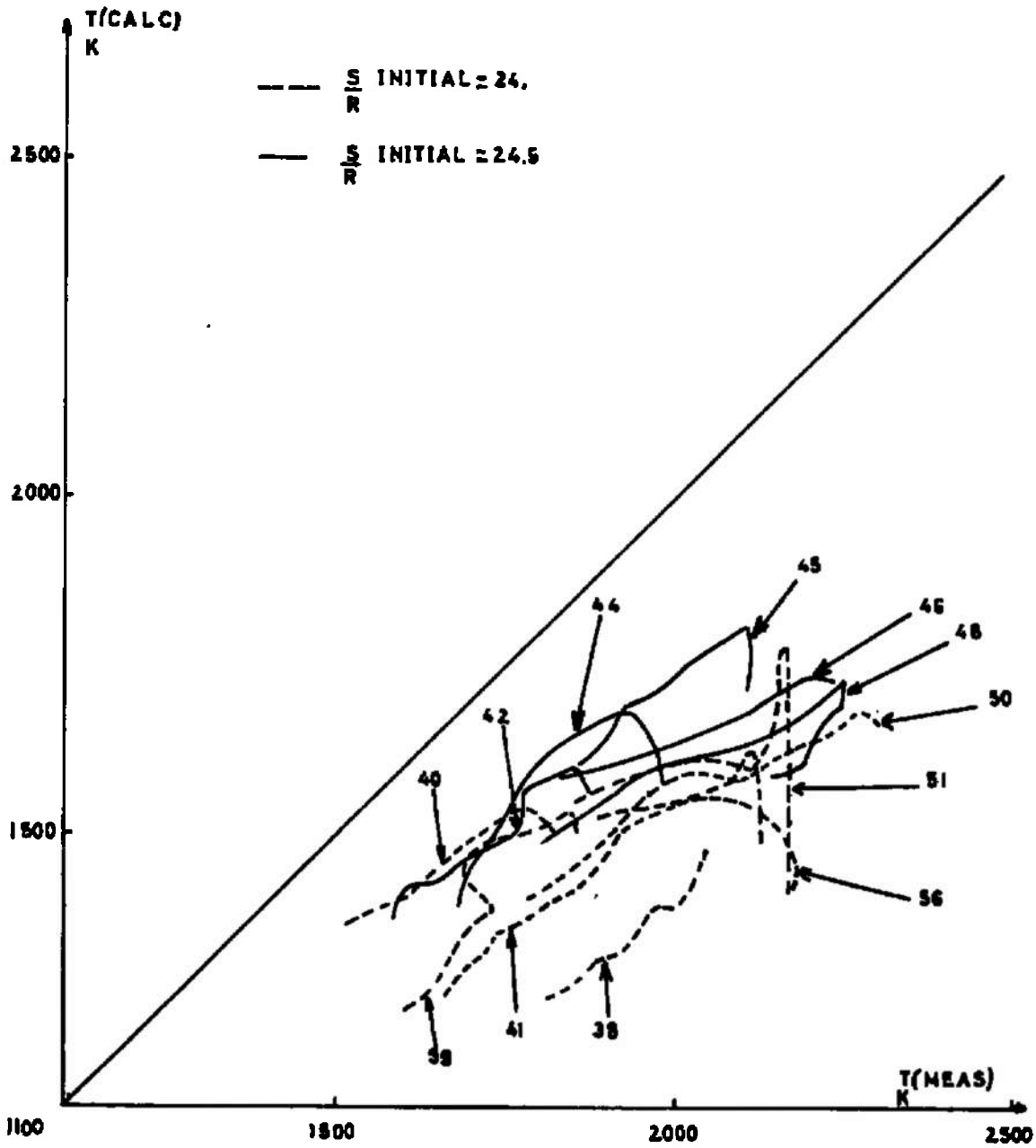


FIG. 30 Summary of T calculated against T measured in air.

An anomaly occurs in temperature measurement of the expansion part of the cycle. At times during the expansion, temperature is found to be increasing whilst pressure and density are decreasing. A possible reason for this anomaly is that the oxygen contained in the air is undergoing a reaction with combustible components (such as with the plastic of the seals) thus changing the composition of the test gas. The results presented in the Figures 24-30 do not include data obtained during the later stages of the expansion.

Because of this doubt regarding the composition of the gas, it is difficult to say at present whether the deviations are due to errors in the experiment or in the equation of state data presented in the AEDC tables (Ref. 17) which was used to obtain the calculated values used in the comparisons.

7. CONCLUSIONS

The compression tube has been shown to be capable of generating samples of test gas up to 3000 Kg/cm^2 and 2300°K . Extensions up to higher temperatures are expected to be possible. It has been shown that the selected instrumentation, piezo-electric transducers, sodium line reversal apparatus and eddy-current distance transducer are suitable in terms of response and accuracy to measure the pressure, temperature and volume in the test time of interest. Careful calibration has enabled overall uncertainty levels below $\pm 5\%$ at peak conditions and typically $\pm 7\%$ to $\pm 10\%$ away from the peak to be attained. One further uncertainty, difficult to quantify, but considered to be small for at least the nitrogen tests is gas contamination. With further refinements, especially in synchronisation of events away from the peak, the uncertainty levels attained could be reduced slightly. Results of tests carried out in a limited entropy range in nitrogen show that agreement to within $\pm 5\%$ with the Enkenhus-Culotta equation of state is achieved below 1400 Kg/cm^2 and 1700 Kg/cm^2 . A gradual deviation to values of 15% is found between experiment and equation of state at higher conditions in nitrogen. The agreement between experiment and equation of state for air is considerably worse than for nitrogen and the trends appear to be reversed. At this stage it has not been verified whether these deviations are due to errors in published tables describing thermodynamic state or associated with contamination problems arising from the use of oxygen used in the experiment.

8. FUTURE EXTENSIONS OF THE RESEARCH

8.1 Interpretation of data

A parameter known fairly accurately, but as yet unused in the comparison with real gas equations of state, is the entropy. The compression is essentially isentropic, such that the initial value of entropy, which can be defined very accurately from the initial running conditions, will remain constant throughout the compression and expansion. A small correction can be made for the energy loss due to heat transfer which has been predicted and measured for several cases. With this redundant piece of information, more insight can be attained as to whether experimental deviations from the equation of state seen so far are experimental errors or true deviations of the equation of state in defining nature. Further numerical routines must be developed to examine the results in this light.

A further redundant parameter whose use could be examined is the knowledge of energy during the compression which could come from accurate calculations and measurements concerning the overall piston cycle e.g. piston motion, friction, heat losses, pressure variation behind the piston, etc.

Further insight into the information can be obtained by fitting measurements to simplified equations of state which give important parameters such as the co-volume term, b , in the Abel-Noble equation.

$$p\left(\frac{1}{\rho} - b\right) = RT$$

and the inter-molecular attractive force term, a , in the Van der Waals equation

$$(p + ap^2)\left(\frac{1}{\rho} - b\right) = RT$$

Also b , in equation of state in virial form for rigid sphere molecules

$$\frac{PV}{RT} = 1 + bp + 0.625 bp^2 + 0.2869 bp^3 + 0.155 bp^4 \dots$$

Furthermore, the parameter Z , can be calculated using

$$Z = \frac{P}{\rho RT}$$

8.2 Extension of experiments to cover a larger temperature and entropy range in nitrogen

Further experiments in nitrogen will be made to extend the experiments of entropy to both higher and lower values, and to increasing the upper limit of the temperature measurements to above 2,500°K to as high as possible below the limiting temperature of the carbon arc source. This will entail gaining experience in the use of the carbon arc light source as a source for the sodium line reversal technique. One result of extending the range to higher temperatures is that smaller volumes of gas are achieved in the test region and hence the uncertainty in ρ will be increased.

8.3 Diagnosis of the large deviations from equation of state of experiments in air

Experiments will be carried out to attempt to determine the cause of the large deviations of the experimental data taken with a test gas of air compared to existing equations of state. Manipulations of the data as described in Section 8.1 will be carried out to aid finding the source of deviation, whether experimental or true errors in defining the equation of state. A spectroscopic study of the test gas during a test is recommended in order to determine the nature of any impurities that may be present. If the study indicates that the deviations are due to experimental errors, then appropriate changes to the experiment will be made where possible such as investigating the use of soft metal seals instead of plastic seals. When satisfactory results are obtained then similar extensions of the experiments will be made as for nitrogen indicated in Section 2.

8.4 Theoretical survey for an appropriate equation of state for air

A literature survey should be carried out to determine an appropriate equation of state for a mixture of gases such as air.

REFERENCES.

1. LUKASIEWICZ : "Experimental Methods of Hypersonics".
2. DAVIDSON : "Statistical Mechanics" Mc Graw Hill. 1962
Chapter 16-20.
3. BEATTIE, J.A. : "Thermodynamic of Real Gases and Mixtures of Real Gases". Thermodynamics and Physics of Matter, Princeton Series on High Speed Aerodynamics and Jet Propulsion. Vol.1, F.D. Rossini Editor, 1955.
4. CULOTTA, S.; ENKENHUS, K.R. : "Analytical Expressions for the Thermodynamic Properties of Dense Nitrogen". VKI TN50 Sept.68
5. RYABININ, Yu, N. : "Gases at High Densities and Temperatures". Pergamon Press Ltd. 1961.
6. LEWIS, M.J.; ROMAN, B.P.; ROUEL, G.P. : "Techniques for Measuring the Thermodynamic Properties of a Dense Gas" VKI TM23 May 1971 or : International Congress on Instrumentation in Aerospace Simulation Facilities : ICIASF 71 Record.
7. LEWIS, M.J. : "A Description of the VKI Piston Driven Shock Tube", VKI TM20, December 1970.
8. GAYDON, A.G.; HURLE, I.R.: "The Shock Tube in High Temperature Chemical Physics". Reinhold Publishing Co., N.Y. 1963.
9. LEWIS, M.J.; TEAGUE, M.J.; MALCOMES-LAWES, D.J.; BERNSTEIN, L. " Production of Free Sodium Atoms for the Spectrum-line Reversal Technique. AIAA Journal. Vol.7, p.1798, Sept.1969.
10. LAPWORTH, K.C. : "Effect of the Laminar Boundary Layer Development in a Shock Tube on Spectrum Line Reversal Temperature Measurements". N.P.L. Aero. Rep. 1060, March 1963.
11. TEAGUE, M.J. : "An Evaluation of the Spectrum line Reversal Technique for Temperature Measurements in Shock Tubes and Tunnels. Ph.D. Thesis, U. of London, England 1968.
12. HENTALL, J.E.; KRAUSE, H.F.; FITE, W.L. : "Transfer of Excitation Energy from Nitrogen Molecules to Sodium Atoms. Disc. of Faraday Soc. 44, p. 157, 1967.
13. NULL, M.R.; LOZIER, W.W. : "The Carbon Arc as a Radiation Standard", Temperature, its Measurement and Control in Science and Industry, Vol 3, Part 1, p.p. 551-558 (Rheinhold Pub. Co)
14. LAPWORTH, K.C.; ALLNUTT, L.A.; PENDLEBURY, J.R.: "Temperature Measurements in Shock Heated Carbon Monoxide by an Infra Red Technique". J. Phys. D; Applied Phys. 1971. Vol.4 p.p.759-768.

15. LAPWORTH, K.C.; QUINN, T.J.; ALLNUTT, L.A.: "A Black Body Source of Radiation Covering a Wavelength Range from Ultra-Violet to the Infra-Red". J. Phys. E. Scientific Instruments 1970, Vol.3 p.p. 116-120.
16. KNOOS, S. : "Theoretical and Experimental Study of Piston Gas-heating with Laminar Energy losses", Northrop Corporate Labs. Hawthorne, California.
17. GRABAU, M.; BRAHINSKY, H.S. : "Thermodynamic Properties of Air from 300 to 6000°K and from 1 to 1000 Amagats". AEDC - TR- 66 - 147. January 1967.
18. GRABAU, M.; BRAHINSKY, H.S. : "Thermodynamic Properties of Nitrogen from 300 to 6000°K and from 1 to 1000 Amagats". AEDC - TR - 66 - 69 August 1966.
19. SCHULTZ, D.L. : "On the Flow in an Isentropic Compression Tunnel". British Aeronautical Research Council ARC 34217, 1973.
20. SCHULTZ, D.L. and JONES : "Heat Transfer Measurements in Short Duration Hypersonic Facilities". AGARDograph 165 February, 1973.
21. ROMAN, B.P.; ROUEL, G.P.; LEWIS, M.J.; RICHARDS, B.E. : "Compression of Medium to High Pressures and Temperatures Using a Ballistic Piston Apparatus". Sept. 1971 VKI Preprint 71.7.